Molecular Therapy
Methods & Clinical Development
Original Article

Mutant allele knockout with novel CRISPR nuclease promotes myelopoiesis in ELANE neutropenia

Peter Sabo,[1,4] Vahagn Makaryan,[1,4] Yosef Dicken,[2] Lital Povodovski,[2] Liat Rockah,[2] Tzlil Bar,[2] Matan Gabay,[2] Dalia Elinger,[2] Ella Segal,[2] Ora Haimov,[2] Maya Antoshvili,[2] Anat London Drori,[2] Tanoya Poulsen,[1] Asael Herman,[2] Rafi Emmanuel,[2,3] and David C. Dale[1,3]

[1]Department of Medicine, University of Washington, Box 356422, 1959 NE Pacific Street, Room AA522, Seattle, WA 98195, USA; [2]EmendoBio, Inc., 400 W 61st Street, #2330, New York NY 10069, USA

Severe congenital neutropenia (SCN) is a life-threatening marrow failure disorder, usually caused by heterozygous mutations in *ELANE*. Potential genetic treatment strategies include biallelic knockout or gene correction via homology-directed repair (HDR). Such strategies, however, involve the potential loss of the essential function of the normal allele product or limited coverage of diverse monogenic mutations within the patient population, respectively. As an alternative, we have developed a novel CRISPR-based monoallelic knockout strategy that precisely targets the heterozygous sites of single-nucleotide polymorphisms (SNPs) associated with most *ELANE* mutated alleles. *In vitro* studies demonstrate that patients' unedited hematopoietic CD34$^+$ cells have significant abnormalities in differentiation and maturation, consistent with the hematopoietic defect in SCN patients. Selective knockout of the mutant *ELANE* allele alleviated these cellular abnormalities and resulted in about 50%–70% increase in normally functioning neutrophils ($p < 0.0001$). Genomic analysis confirmed that *ELANE* knockout was specific to the mutant allele and involved no off-targets. These results demonstrate the therapeutic potential of selective allele editing that may be applicable to SCN and other autosomal dominant disorders.

INTRODUCTION

Severe congenital neutropenia (SCN) is a rare, life-threatening hematopoietic disorder characterized by a paucity of mature neutrophils.[1,2] SCN patients typically present within the first 6 months of life with recurrent, occasionally life-threatening infections attributable to a selective defect in neutrophil production.[3]

The most frequent causes of SCN (45%–88% according to the inclusion criteria and cohort used in the report) are more than 100 different autosomal dominant mutations in the *ELANE* gene encoding neutrophil elastase (NE).[1,3–8] The molecular pathways that underlie *ELANE*-associated neutropenia are complex and not fully understood.[4,9] One possible mechanism is the misfolding of mutant NE, which is improperly processed, resulting in aberrant intracellular localization. Cytoplasmic aggregation of mutant NE induces endoplasmic reticulum (ER) stress and the unfolded protein response, eventually leading to maturation arrest, i.e., a robust marrow that produces only a few metamyelocytes, bands, and mature neutrophils.[1,10]

Currently, SCN patients can be treated effectively, long term, with daily injections of granulocyte colony-stimulating factor (G-CSF).[11] However, such patients continue to be at risk of evolution to myelodysplastic syndromes (MDS) and acute myeloid leukemia (AML).[1,6,12–14] To date, the only alternative treatment available is allogeneic hematopoietic stem cell transplantation (HSCT),[15] which requires matched donors and can lead to graft-versus-host disease and serious fatal infections.[16,17] Thus, there is a great interest in new and more efficient treatments.

Biallelic knockout of *ELANE* alleles (both mutant and wild type) has been suggested by some groups as a potential treatment for *ELANE*-mediated SCN. Studies have shown that complete *ELANE* knockout in SCN patient-derived HSCs resolves the maturation arrest and results in normal neutrophil differentiation *in vitro*.[18–20] However, removal of both *ELANE* alleles dampens the levels of NE, a protein highly involved in host immune defenses[21–28] and recently reported to attenuate tumor growth.[29]

Recently, Tran et al. used the CRISPR-Cas9 system and a DNA donor template to initiate homology-directed repair (HDR) of a mutated *ELANE* gene.[30] Although promising, this approach poses several

Received 13 December 2021; accepted 3 June 2022;
https://doi.org/10.1016/j.omtm.2022.06.002.

[3]Senior author

[4]These authors contributed equally

Correspondence: Rafi Emmanuel, EmendoBio, Inc., 400 W 61st Street, #2330, New York, NY 10069, USA. .
E-mail: rafi@emendobio.com
Correspondence: David C. Dale, Professor of Medicine ,University of Washington, Box 356422, 1959 NE Pacific Street, Room AA522, Seattle, WA 98195 .
E-mail: dcdale@uw.edu

This is an open access article under the CC BY-NC-ND license (http://creativecommons.org/licenses/by-nc-nd/4.0/).

A

SNP ID	Heterozygosity frequency	
	Healthy population	Patient population
rs10414837	33%	43%
rs3761005	46%	45%
rs1683564	42%	42%

B

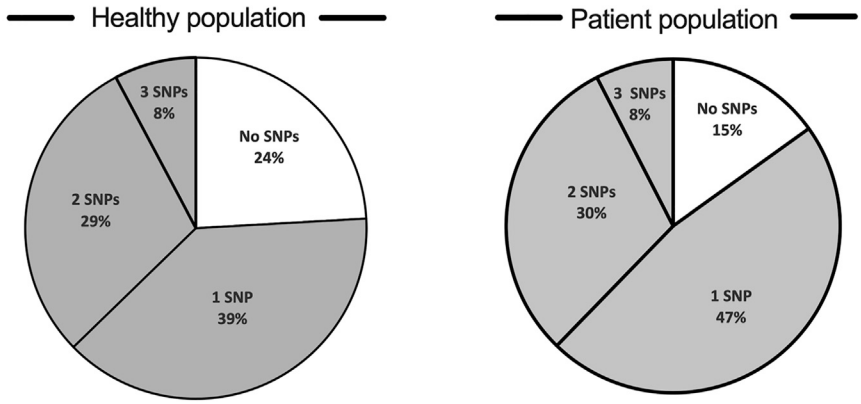

Figure 1. Heterozygosity frequency and coverage of patient and healthy populations by the three SNPs

(A) Heterozygosity frequency of each of the three chosen SNPs in the healthy (left) and patient (right) populations. Heterozygosity frequency was similar among the healthy and patient populations for each of the three SNPs. rs10414837, p = 0.126, odds ratio = 0.653; rs3761005, p = 0.9615, odds ratio = 1.014; rs1683564, p = 0.9475, odds ratio = 1.019; all analyzed by chi-square. (B) Pie chart presenting the percentages of the population being heterozygous for at least one of the three chosen SNPs (gray) in the healthy (left) or patient (right) population. The healthy and patient populations are covered similarly by the three SNPs (more than 75%, p = 0.1285, odds ratio = 0.56, chi-square).

challenges.[31–33] HDR-based gene editing targets specific mutations. Given the numerous mutations associated with SCN,[1,4] mutation-specific targeting approaches are relevant to only a minor portion of the patient population.

In addition, successful gene correction in hematopoietic stem cells (HSCs) is often achieved *in vitro*, but some studies have reported a limited long-term reconstitution of edited HSCs *in vivo*.[34]

In this study we present a CRISPR-based potential gene therapy that provides specific knockout of an *ELANE* mutant allele while preserving the functional wild-type allele. Monoallelic knockout in SCN patient-derived HSCs, using an optimized high-fidelity nuclease, resolves maturation arrest and restores neutrophil differentiation. The target sites for such a unique knockout strategy are single-nucleotide polymorphisms (SNPs) that are frequently heterozygous in the SCN patient population and are linked to the majority of *ELANE* mutations. Thus, this approach could provide a feasible treatment to more than about 75% of *ELANE*-mediated SCN patients and potentially serve as a model for treatment of other autosomal dominant disorders.

RESULTS

Representative *ELANE* mutations and respective therapeutic strategies

SCN is associated with numerous heterozygous mutations in *ELANE*. The current study presents a novel approach for knockout of the mutated *ELANE* allele by targeting heterozygous sites of SNPs that are adjacent to the majority of *ELANE*-mediated SCN mutations, instead of independently editing each pathogenic mutation. Of hundreds of potential SNPs in the *ELANE* gene, we identified three SNPs (termed herein rs1683564, rs10414837, and rs3761005), retrieved from the healthy database of the 1000 Genomes Project Consortium, that are frequently heterozygous in the healthy population. Analysis of the healthy and patient populations revealed similar heterozygosity frequencies between the two populations for each of the SNPs (Figure 1A). About 76%–85% of each of the populations (healthy and patient, respectively) was heterozygous in at least one of the SNPs, indicating the applicability of our strategy to more than about 75% of the SCN patient population (Figure 1B and Table S1). For each of the three SNPs, located along the abundant clusters of *ELANE* mutations (Figure 2A and Figure 2B, top), we developed an editing ribonucleoprotein (RNP) composition that includes two different guides and an optimized CRISPR-associated nuclease termed OMNI A1 V10 (discovery and engineering of the nuclease are described in the supplemental information). One guide (termed herein sgRNA constant) is common to all three compositions and cuts both *ELANE* alleles at intron 4. The editing at the intron site did not affect exons 4 and 5 or any of the regulatory elements within the intron (Figure S1). The second guide targets the heterozygous form of one of the three SNPs and therefore cuts only one allele. The composition that targets SNP rs1683564 excises exon 5 and the entire 3′ UTR, causing the degradation of the destabilized mRNA transcript (Figure 2B [I]). The compositions that target either SNP rs10414837 or SNP rs3761005 (Figure S2) lead to excision of most of the coding region and the promotor, thus preventing the transcription of the mutated allele (Figure 2B [II and III]). The current study is focused on composition I, targeting the rs1683564 SNP. The more prevalent form of rs1683564 SNP is cytosine and is referred to herein as the reference (ref) allele. Adenosine is the less prevalent form of the SNP and is referred to herein as the alternative (alt) allele. Prior to treatment,

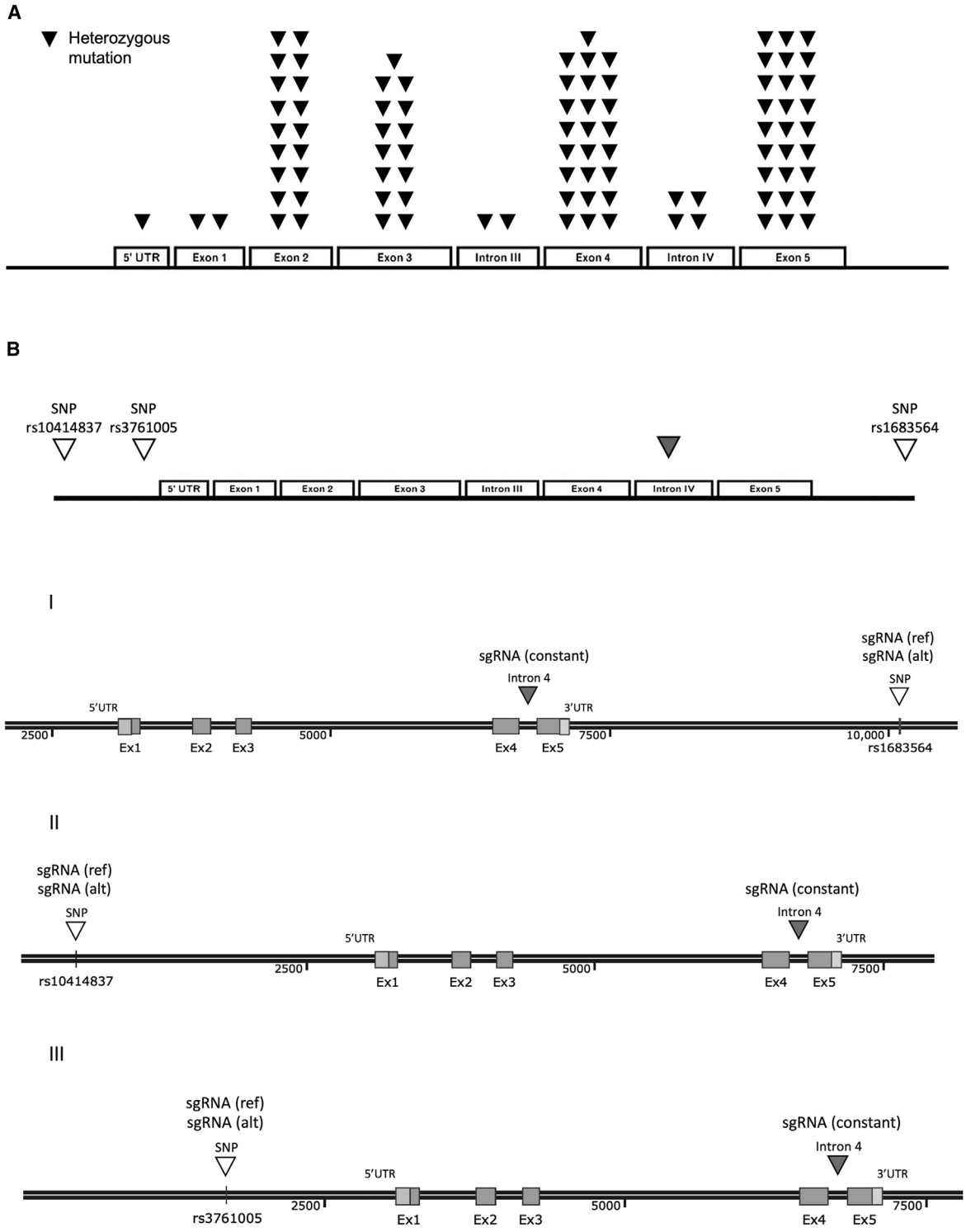

Figure 2. Schematic of representative *ELANE* mutations and suggested therapeutic strategies

(A) Linear representation of *ELANE*'s five exons and four introns showing locations of representative heterozygous mutations associated with SCN depicted as black inverted triangles. Based on Makaryan et al.[4] (B) Schematics of three identified SNPs (white inverted triangles) associated with the majority of *ELANE* mutations and a common cut site (gray inverted triangle), based on which three allele-specific sgRNA guides and a constant guide were designed representing three monoallelic excision strategies.

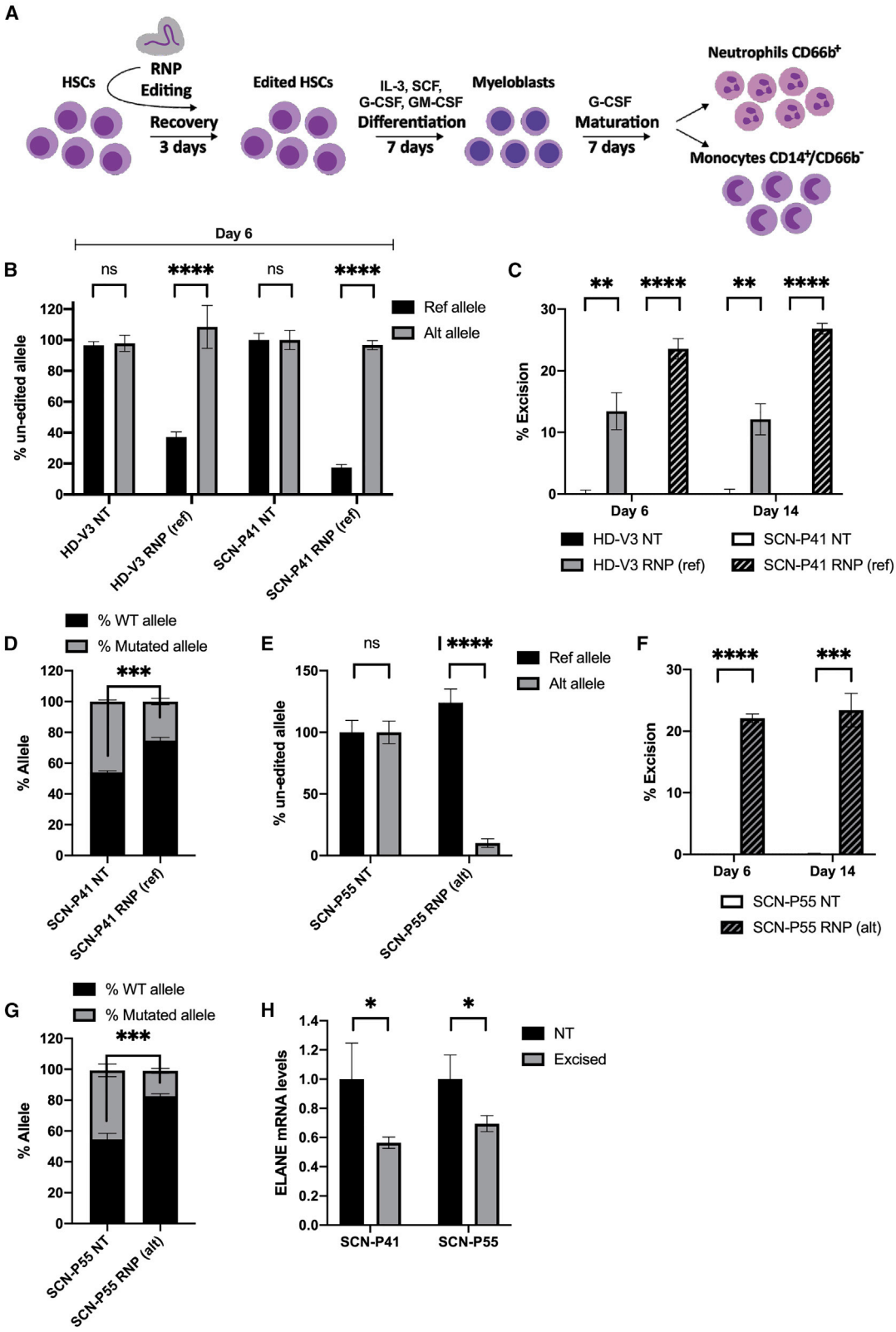

(legend on next page)

patient cells are genotyped to determine if the mutation and the SNP are on the same allele or different alleles in a process termed linkage determination (Figure S3). If the pathogenic mutation is linked to the reference allele, a nuclease-guide RNA composition including a guide (sgRNA(ref)) that targets the cytosine form of the SNP is chosen (termed herein RNP(ref)). If the pathogenic mutation is linked to the alternative allele, a composition including a guide (sgRNA(alt)) that targets the adenosine form of the SNP is chosen (termed herein RNP(alt)). The guides differ by only one nucleotide and when used with the sgRNA constant result in the same editing outcome (Figure S4).

Allele specificity and excision efficiency using OMNI A1 V10 nuclease in an SNP-based knockout strategy

Unlike most CRISPR-associated editing strategies that cut the target gene in both alleles, our approach is directed at knockout of the mutated allele while keeping the wild-type functional allele intact. To demonstrate the feasibility of our monoallelic editing strategy, HSCs heterozygous to SNP rs1683564, taken from healthy donors and SCN patients, were excised using either RNP(ref) or RNP(alt) (according to their linkage) or left non-treated (NT). HSCs recovered for 3 days in $CD34^+$ expansion medium; then were cultured for 7 days in the presence of IL-3, SCF, GM-CSF, and G-CSF for proliferation and myeloid progenitor differentiation; and subsequently were stimulated with G-CSF for a further 7 days for neutrophil differentiation (Figure 3A).

A fraction of the cells was harvested at days 6 and 14 of differentiation for genomic DNA or RNA extraction. Allele specificity was determined at day 6 of differentiation by two competitive probes binding either the alternative allele or the reference allele (for probes' specificity see supplemental information and Figure S5). To test the RNP(ref) composition we used HSCs from SCN patient P41 (SCN-P41) harboring a mutation on the reference allele and HSCs from healthy donor V3 (HD-V3), both heterozygous to the reference form of the SNP. Digital Droplet PCR (ddPCR) revealed that editing using RNP(ref) was specific, as only about 40% and about 20% of the reference allele remained intact in HSCs of HD-V3 and SCN-P41, respectively (Figure 3B). The alternative allele, however, was not affected by the RNP(ref) composition, as indicated by its high levels, which were similar to those of NT cells (Figure 3B). These results demonstrated that treatment with the RNP(ref) composition leads to allele-specific editing.

Next, we evaluated excision efficiency at days 6 and 14 of neutrophil differentiation. Excision was determined by amplification of two regions in *ELANE* using two differently labeled probes, one for exon 1, which is not affected by the current excision strategy, and a second probe for exon 5, which is degraded upon excision (Figure 2B [I]). The ratio between the signals of the two probes was translated to excision efficiency. Treatment with RNP(ref) resulted in about 13% excision in HSCs of HD-V3 and about 25% excision in HSCs of SCN-P41 (Figure 3C). Given the high specificity of the nuclease (Figure 3B), this excision correlated to about 50% of the cell population that had undergone excision at the reference allele in HSCs of SCN-P41. RNP(ref) treatment also involved about 6% inversion events in HSCs of SCN-P41 as measured by EvaGreen staining (Figures S6A and S6B). Of note, other experiments evaluating RNP(ref)-mediated excision levels in HSCs from healthy donors showed higher excision levels than reported above that were comparable to those measured in HSCs of SCN-P41 (Figure S7). In addition, next-generation sequencing (NGS) analysis of cDNA from SCN-P41 cells targeting exon 4 harboring a mutation showed a 1:1 ratio between wild-type and mutated alleles in NT cells. RNP(ref) treatment shifted the wild-type-to-mutated allele ratio to 3:1 by differentially reducing the mutated allele transcript, thereby enriching the wild-type allele (Figure 3D).

To evaluate the specificity and efficiency of the RNP(alt) composition, we used HSCs from SCN patient P55 (SCN-P55) harboring a mutation on the alternative allele and heterozygous to the alternative form of the SNP. RNP(alt)-based treatment resulted in editing of about

Figure 3. Allele specificity and excision efficiency of OMNI A1 V10 nuclease compositions

(A) Scheme depicting experimental workflow. HSCs from healthy donors and SCN patients were electroporated with RNPs or left non-treated followed by 3 days of recovery in $CD34^+$ expansion medium. Cells were then subjected to differentiation by culturing for 7 days with IL-3, SCF, GM-CSF, and G-CSF for proliferation and myeloid progenitor differentiation, followed by a 7-day culture in G-CSF for neutrophil differentiation. (B) Bar graph representing percentages of un-edited reference (black) and alternative (gray) alleles at day 6 of differentiation in HSCs taken from either a healthy donor (HD-V3) or an SCN patient (SCN-P41) and treated with RNP(ref) composition or left non-treated (NT), as measured by ddPCR (n = 3 groups of cells from HD-V3 healthy/SCN-P41 patient donors). Statistical significance is indicated by ****$p < 0.0001$; ns, not statistically significant. (C) Bar graph representing percentages of excision at days 6 and 14 of differentiation in HSCs taken from either a healthy donor (HD-V3) (non-treated [NT, black] or RNP(ref)-treated [gray]) or an SCN patient (SCN-P41) (NT [white] or RNP(ref)-treated [hatched]), as measured by ddPCR (n = 3 groups of cells from HD-V3 healthy/SCN-P41 patient donors). Statistical significance is indicated by **$p < 0.01$, ****$p < 0.0001$. (D) Bar graph representing percentages of wild-type (black) and mutated (gray) alleles in cDNA taken from SCN-P41 patient HSCs that were either RNP(ref)-treated or left NT, as measured by NGS targeting the mutation site (n = 3 groups of cells from patient SCN-P41). Statistical significance is indicated by ***$p < 0.001$. (E) Bar graph representing percentages of unedited reference (black) and alternative (gray) alleles at day 6 of differentiation in HSCs taken from an SCN patient (SCN-P55) treated with RNP(alt) composition or left NT, as measured by ddPCR (n = 3 groups of cells from patient donor SCN-P55). Statistical significance is indicated by ****$p < 0.0001$; ns, not statistically significant. (F) Bar graph representing percentages of excision at days 6 and 14 of differentiation in HSCs taken from an SCN patient (SCN-P55): NT (white) or RNP(alt)-treated (hatched), as measured by ddPCR (n = 3 groups of cells from patient donor SCN-P55). Statistical significance is indicated by ***$p < 0.001$,****$p < 0.0001$. (G) Bar graph representing percentages of wild-type (black) and mutated (gray) alleles in cDNA taken from patient SCN-P55 HSCs that were either RNP(alt)-treated or left NT, as measured by NGS targeting the mutation site (n = 3 groups of cells from patient SCN-P55). Statistical significance is indicated by ***$p < 0.001$. (H) Bar graph representing *ELANE* mRNA levels in day 6 differentiated HSCs of patients SCN-P41 and SCN-P55 that were either NT (black) or RNP(ref)/RNP(alt)-treated, respectively (excised, gray). Data are presented relative to the NT group (n = 3 groups of cells from patients SCN-P41 and SCN-P55). Statistical significance is indicated by *$p < 0.05$. Bars represent mean values with standard deviation.

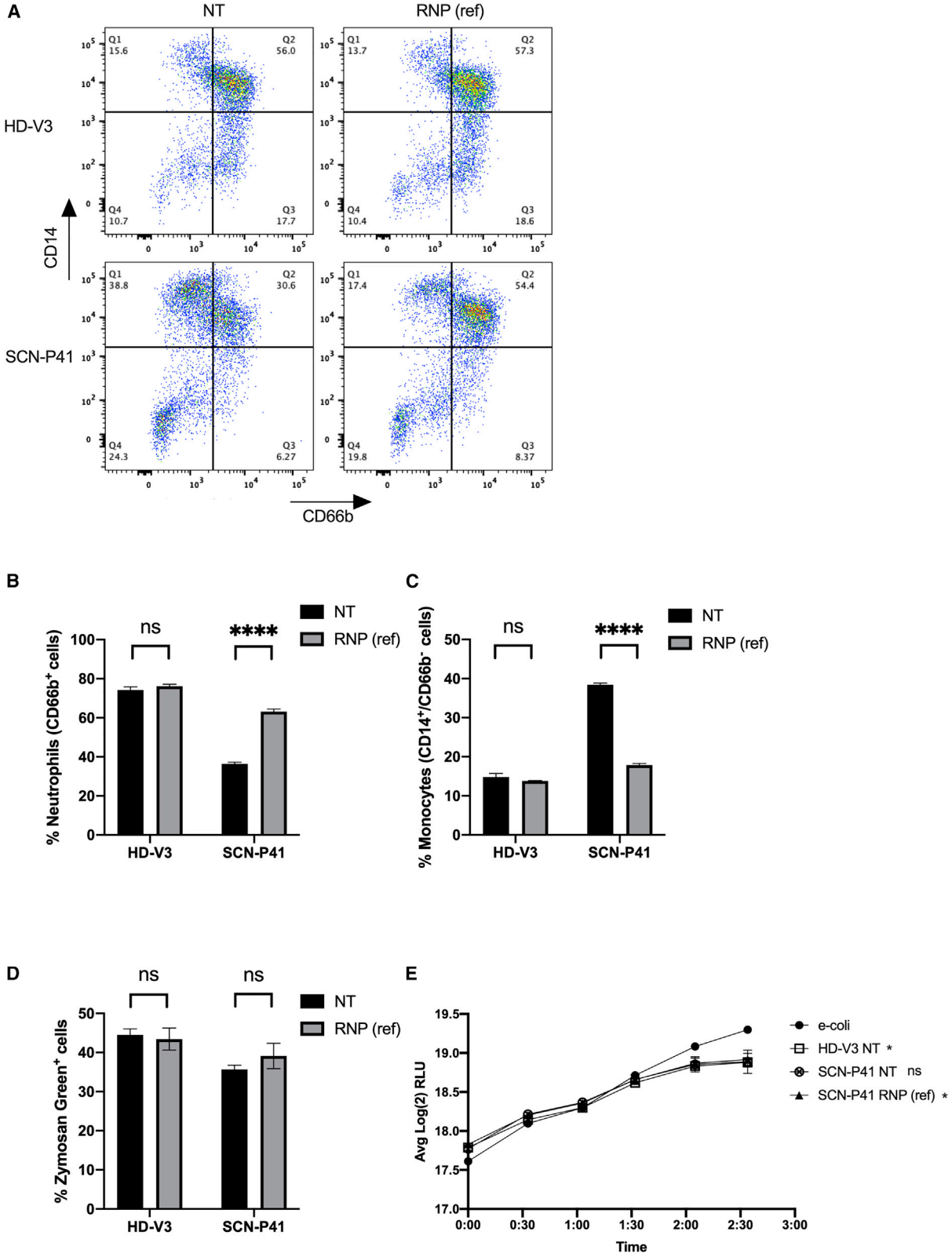

(legend on next page)

90% of the alternative allele (only 10% remained intact), whereas the reference allele was kept intact at day 6 of differentiation (Figure 3E). Excision levels in SCN-P55 HSCs were about 23% at days 6 and 14 of neutrophil differentiation (Figure 3F), indicating that about 46% of the cell population had undergone excision at the alternative allele. RNP(alt) treatment resulted in 7.6% inversion events in SCN-P55 HSCs as measured by EvaGreen staining (Figure S6C). Specificity and excision efficiency of RNP(alt)-edited HSCs of healthy donors were tested and found comparable to those obtained in patient-derived cells (Figure S7). In addition, NGS analysis of cDNA from SCN-P55 cells targeting exon 5 harboring a mutation showed enrichment of the wild-type allele (Figure 3G). *ELANE* mRNA levels were decreased following excision in cells from patients SCN-P41 and SCN-P55 (Figure 3H). In view of the increased wild-type:mutant allele ratio obtained following excision (Figures 3D and 3G), the reduced mRNA levels were mainly a result of the degradation of the mutated transcript.

Next, we confirmed that RNP(alt)-based excision had occurred in a sub-population of HSCs ($CD34^+/CD90^+$ cells) that is considered essential for multilineage engraftment and hematopoietic reconstitution[35] (Figure S8). An unbiased survey (GUIDE-seq) of whole-genome off-target cleavage using OMNI A1 V10 nuclease and each of constant guide (SgRNA(constant)), reference guide (SgRNA(ref)), and alternative guide (SgRNA(alt)) resulted in no identified off-targets ($\leq$4 mismatches) (Figures S9A–S9C and Table S2). In addition, *in silico* off-target analysis was performed for each of the guides and identified a few potential off-targets. None of these off-targets were validated by a rhAmpSeq analysis done on edited HSCs from patients SCN-P41 and SCN-P55 (Figure S9D), demonstrating the high fidelity of the nuclease compositions. Taken together, the results provided above present an active, highly accurate nuclease that can target the mutant allele while preserving the intact wild-type functional allele.

OMNI A1 V10-facilitated editing boosts neutrophil differentiation and maturation *in vitro*

To demonstrate the functional outcome of our SNP-based single-allelic editing approach we evaluated neutrophil differentiation and maturation capacities of RNP(ref)-edited and NT healthy and patient-derived HSCs *in vitro*, at day 14 of differentiation. Flow cytometric analysis showed that about 74% of the HD-V3 HSCs, subjected to the differentiation protocol differentiated into neutrophils ($CD66b^+$; two right quarters [Q2 + Q3] of the dot plot), compared with only 36% of the SCN-P41-derived HSCs. In contrast, only about 15% of HD-V3 HSCs differentiated into monocytes ($CD14^+/CD66b^-$; upper left quarter [Q1] of the dot plot) compared with 38% of the SCN-P41-derived HSCs. These observations are consistent with the characteristic hematopoietic defect in SCN patients (Figures 4A–4C; NT: HD-V3 versus SCN-P41). SCN-P41-derived HSCs treated with RNP(ref) showed a 74% increase in neutrophils ($CD66b^+$ cells) and a 2-fold reduction in the monocytic subset ($CD14^+/CD66b^-$) (Figures 4A–4C; SCN-P41: NT versus RNP(ref)). A similar increase in neutrophil count was observed in SCN-P41-derived edited HSCs by flow cytometric analysis of $CD11b^+/CD15^+$ cells (Figures S10A and S10B). RNP(ref)-mediated editing in HSCs of HD-V3 did not affect the monocytic and neutrophilic subsets, supporting the safety of this composition (Figures 4A–4C; HD-V3: NT versus RNP(ref)). After demonstrating that our allele-specific editing approach significantly improved the cellular abnormalities associated with SCN, we next assessed neutrophilic functions in RNP(ref)-treated and NT healthy (V3) and patient (P41) HSC-derived neutrophils. *In vitro* phagocytic capacity was tested by measurement of phagosomal uptake of zymosan green particles by neutrophils from the different groups. Flow cytometric analysis revealed equivalent levels of phagocytosis in RNP(ref)-treated and NT neutrophils from both HD-V3 and SCN-P41 (Figure 4D). In addition, anti-bacterial killing capacity was examined by incubating neutrophils derived from NT healthy (HD-V3) and patient (SCN-P41) HSCs and RNP(ref)-treated patient HSCs (SCN-P41, RNP(ref)) with *E. coli* bacteria expressing the bacterial luciferase gene and tracking real-time changes in light emission, expressed as relative light units (RLUs). Healthy NT, RNP(ref)-treated, and NT patient-derived neutrophils exhibited efficient bacterial killing, as indicated by a 23%–25% decrease in bacterial unit (RLU) relative to the bacteria-only control (Figure 4E). The SCN-P41 NT group showed reduced bacterial units, although not statistically different from the bacteria-only control group.

An experiment using the RNP(ref) composition was conducted on cells from another patient (SCN-P42) and gave similar excision, differentiation, and functional results, including histological staining demonstrating the restoration of neutrophil differentiation (Figure S11). Thus, specific knockout of the *ELANE* mutated allele by RNP(ref) composition ameliorated the aberrant phenotype of

Figure 4. RNP(ref)-facilitated editing boosts neutrophil differentiation and maturation *in vitro*

(A) Representative fluorescence-activated cell sorting (FACS) plots of non-treated (NT, left) and RNP(ref)-treated (right) healthy donor (HD-V3, top) and patient SCN-P41 (bottom) differentiated HSCs, analyzed for neutrophilic ($CD66b^+$) and monocytic ($CD14^+/CD66b^-$) subsets. (B) Quantitative analysis of respective FACS data for percentages of neutrophils ($CD66b^+$ cells) in healthy (HD-V3) and SCN patient (SCN-P41) differentiated HSCs that were NT (black) or treated with RNP(ref) (gray) (n = 3 groups of cells from HD-V3 healthy/SCN-P41 patient donors). Statistical significance is indicated by ****$p < 0.0001$; ns, not statistically significant. (C) Quantitative analysis of respective FACS data for percentages of monocytes ($CD14^+/CD66b^-$ cells) in healthy (HD-V3) and SCN patient (SCN-P41) differentiated HSCs that were NT (black) or treated with RNP(ref) (gray) (n = 3 groups of cells from HD-V3 healthy/SCN-P41 patient donors). Statistical significance is indicated by ****$p < 0.0001$; ns, not statistically significant. (D) Quantification of percentages of zymosan green uptake by healthy (HD-V3) and SCN patient (SCN-P41) differentiated HSCs that were NT (black) or treated with RNP(ref) (gray). ns, not statistically significant. (E) Graph depicts real-time change in light emission, in relative light units (RLUs), from 200,000 luciferase-expressing bacterial cells incubated with differentiated neutrophils from healthy NT (HD-V3; square), patient NT (SCN-P41; crossed circle), or patient RNP(ref)-treated (SCN-P41, RNP(ref); triangle) HSCs compared with bacterial cells-only control (e-coli; circle). Statistical significance for each of the groups versus the *E. coli* control at the last time point presented, when RLU levels reached plateau, is indicated by *$p < 0.05$; **$p < 0.01$; ns, not statistically significant. Bars represent mean values with standard deviation.

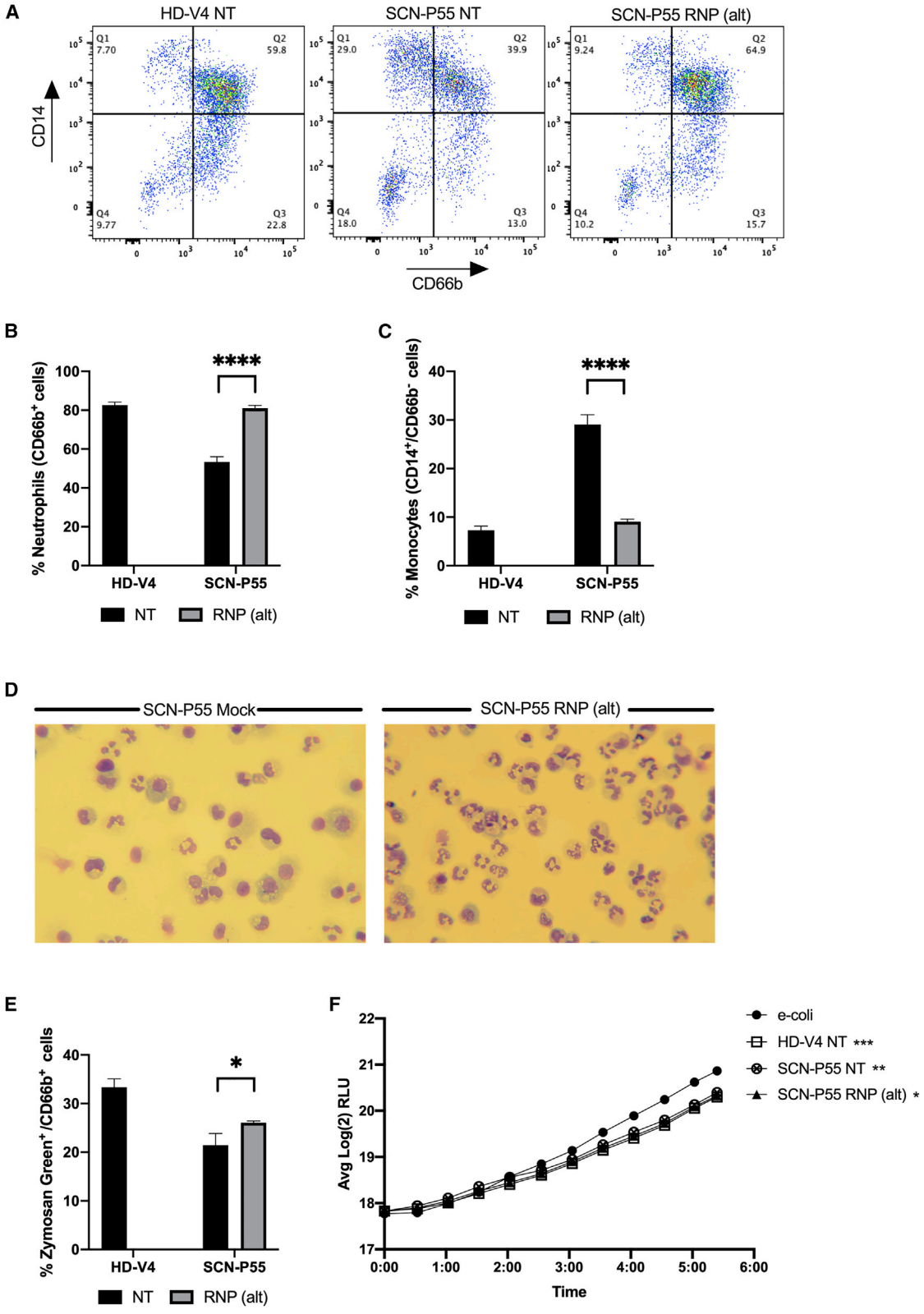

(legend on next page)

attenuated differentiation toward neutrophils while preserving essential neutrophil functions. A similar analysis was performed on the RNP(alt) composition. Flow cytometric analysis showed that about 83% of HD-V4-derived HSCs differentiated into neutrophils ($CD66b^+$; two right quarters [Q2 + Q3] of the dot plot) and about 7% differentiated into monocytes ($CD14^+/CD66b^-$; upper left quarter [Q1] of the dot plot). SCN-P55-derived HSCs showed a lower differentiation toward neutrophils (about 53%) and a higher differentiation to monocytes (about 29%) (Figures 5A–5C; NT: HD-V4 versus SCN-P55), representing a typical SCN hematopoietic defect. SCN-P55-derived HSCs treated with RNP(alt) presented a 1.5-fold increase in neutrophils ($CD66b^+$ cells) and a 3-fold reduction in the monocytic subset ($CD14^+/CD66b^-$) (Figures 5A–5C; SCN-P41: NT versus RNP(alt)). A similar increase in neutrophil subset was observed in SCN-P55-derived edited HSCs by flow cytometric analysis of $CD11b^+/CD15^+$ cells (Figures S10C and S10D). Diff-Quik staining of SCN-P55-derived HSCs treated with RNP(alt) or electroporated without a nuclease composition (SCN-P55 Mock) revealed higher numbers of cells with classical polymorphonuclear neutrophilic morphology in the RNP(alt)-treated group compared with the mock group (Figure 5D). Flow cytometric analysis of zymosan green particles revealed slightly higher levels of phagocytosis in RNP(alt)-treated neutrophils compared with NT neutrophils from SCN-P55 (Figure 5E). In addition, healthy NT (HD-V4), patient NT (SCN-P55), and RNP(alt)-treated (SCN-P55, RNP(alt)) neutrophils exhibited efficient bacterial killing, as indicated by a significant 30% decrease in bacterial unit (RLU) relative to the bacteria-only control (Figure 5F). A classical pathogen-killing mechanism of neutrophils is the formation of neutrophil extracellular traps (NETs). We therefore confirmed that our excision strategy does not compromise NETosis capacity (Figure S12).

An experiment using the RNP(alt) composition was conducted on cells from another patient (SCN-P12) and showed similar excision, differentiation, and functional results (Figure S13). Moreover, another experiment performed on patient cells (SCN-P56) harboring a mutation on exon 2, located upstream of the mutations found in previous patients (exons 4 and 5), showed similar results (Figure S14). The results described herein indicate that a single-allelic knockout of an *ELANE* mutated allele, using RNP(ref) and RNP(alt) nuclease compositions, is effective and safe both in boosting neutrophil differentiation and in maintaining essential neutrophilic core functions.

DISCUSSION

The prognosis of most SCN patients has been dramatically improved following the introduction of G-CSF therapy, owing to the increase in absolute neutrophil counts and a reduced incidence of infections.[1] Nonetheless, patients on long-term G-CSF treatment remain at risk of hematological complications, especially those who respond poorly to this treatment or require high daily doses of G-CSF.[6,12–14] G-CSF therapy induces compensatory mechanisms of granulopoiesis, but does not treat the etiological roots of the disease. Moreover, the full functions of neutrophils in SCN patients on G-CSF therapy may not be completely restored, which may account for the complications still observed in treated patients.[1,12,13,36]

The most frequent causes of SCN are heterozygous mutations in the *ELANE* gene encoding NE.[4,37,38] *ELANE* mutations are characterized by their dominant nature, resulting in the development of neutropenia despite the presence of one intact wild-type *ELANE* allele.[8,37,39,40] The pathophysiological pathways that underlie neutrophil maturation arrest may vary depending on which elastase domain was affected by the mutation.[41,42] However, a common possible etiology relates to the production of an abnormal NE that cannot be folded, secreted, or degraded, resulting in its intracellular accumulation and mislocalization. These events induce ER stress and the unfolded protein response, leading to increased apoptosis of neutrophil precursors.[9,43–45] Moreover, co-expression of the mutant and wild-type forms of NE within the same cell results in inhibition of the wild-type NE activity.[41] Thus, a desired therapy, as proposed in the current study, would be one that specifically removes the mutated allele, thereby preventing the destructive cascade of events initiated by abnormal NE, but at the same time preserves the wild-type *ELANE* allele, intact and functional.

Recently, Nasri et al. demonstrated that CRISPR-Cas9-mediated *ELANE* gene deletion in cells from SCN patients harboring *ELANE* mutations increased neutrophil differentiation and maturation *in vitro*. The study reported that the resulting neutrophils retained phagocytic, oxidative, and chemotactic functions.[19] However, such

Figure 5. RNP(alt)-mediated editing promotes HSC differentiation toward functional neutrophils *in vitro*

(A) Representative FACS plots of non-treated healthy donor (HD-V4 NT, left), NT SCN patient (SCN-P55, middle), and RNP(alt)-treated SCN patient (right) differentiated HSCs, analyzed for neutrophilic ($CD66b^+$) and monocytic ($CD14^+/CD66b^-$) subsets. (B) Quantitative analysis of respective FACS data for percentages of neutrophils ($CD66b^+$ cells) in differentiated HSCs from NT healthy donor (HD-V4; black) and SCN patient (SCN-P55) either NT (black) or treated with RNP(alt) (gray) (n = 3 groups of cells from HD-V4 healthy/SCN-P55 patient donors). Statistical significance is indicated by ****$p < 0.0001$. (C) Quantitative analysis of respective FACS data for percentages of monocytes ($CD14^+/CD66b^-$ cells) in differentiated HSCs from NT healthy donor (HD-V4; black) and SCN patient (SCN-P55) either NT (black) or treated with RNP(alt) (gray) (n = 3 groups of cells from HD-V4 healthy/SCN-P55 patient donors). Statistical significance is indicated by ****$p < 0.0001$. (D) Diff-Quik staining of P55 SCN patient-derived differentiated HSCs treated with RNP(alt) or electroporated without a nuclease composition (SCN-P55 Mock). Microphotographs were taken on a Leitz Laborlux S polarizing light microscope at 400× magnification using a Nikon DSLR digital camera. (E) Quantification of percentages of zymosan green uptake by differentiated HSCs from NT healthy donor (HD-V4; black) and SCN patient (SCN-P55) either NT (black) or treated with RNP(alt) (gray) (n = 3 groups of cells from HD-V4 healthy/SCN-P55 patient donors). Statistical significance is indicated by *$p < 0.05$. (F) Graph depicts real-time change in light emission in relative light units (RLUs) from 200,000 luciferase-expressing bacterial cells incubated with differentiated neutrophils from healthy NT (HD-V4; square) HSCs, patient NT (SCN-P55; crossed circle), and patient RNP(alt)-treated (SCN-P55, RNP(alt); triangle) HSCs compared with bacterial cells-only control (e-coli; circle). Statistical significance for each of the groups versus *E. coli* control at the last time point presented, when RLU levels reached plateau, is indicated by *$p < 0.05$, **$p < 0.01$, and ***$p < 0.001$. Bars represent mean values with standard deviation.

an approach could be counterproductive, as it completely eliminates expression of NE, which has been reported to mediate a non-redundant role in innate immune defense against pathogens. Deficiency in NE results in increased susceptibility to sepsis and death following infection in gram-negative bacteria.[23,24] NE targets bacterial virulence proteins, modulates inflammatory cytokines, and degrades bacterial outer-membrane proteins.[21,25–27,46,47] In addition, NE has an essential fungicidal activity.[22]

Another mechanism by which neutrophils kill bacteria, fungi, and parasites is the formation of NETs. Upon pathogen recognition, NE is released from the neutrophil's granules and translocates to the nucleus, where it degrades histones and promotes chromatin decondensation. The chromatin expands, leading to cell rupture and the release of web-like chromatin fibers that trap and kill pathogens.[48] Papayannopoulos et al. demonstrated that chromatin decondensation is blocked by specific pharmacological inhibitors of NE and that NE knockout animals do not form NETs, and their neutrophils exhibit condensed nuclei, in an *in vivo* mouse model of lung infection.[48] Interestingly, our allele-specific excision strategy, which keeps the wild-type NE intact, resulted in preservation of NETosis capacity. Taken together, the abundant published experimental data unequivocally attribute to NE essential non-redundant roles. Therefore, strategies aimed at eliminating NE must be reevaluated, considering its beneficial functions.

Further support for the need to preserve functional NE comes from a recent study identifying the anti-cancer properties of this protein. The study reported that NE attenuates primary tumor growth and produces a $CD8^+$ T-cell-mediated abscopal effect to attack distant metastases. NE selectively induces DNA damage and promotes apoptosis in cancer cells while sparing non-cancer cells. Interestingly, this effect is attenuated *in vivo* due to the presence of serine protease inhibitors that limit NE activity, resulting in protection and prosperity of cancer cells.[29] Thus, complete removal of NE could have detrimental consequences. In alignment with this finding, there are no examples of healthy individuals carrying a biallelic *ELANE* knockout,[49] while naturally occurring single-allele knockout exists in healthy people.[50] Notably, allele-specific knockout is a desired therapeutic goal, not only in SCN, but also in other autosomal dominant disorders, as was recently demonstrated for Huntington's disease.[51]

In view of the importance of keeping a functional copy of *ELANE*, we suggest a unique approach for targeting SCN-related *ELANE* mutated alleles while sparing the wild-type allele. Such an approach employs a composition, consisting of a CRISPR-associated nuclease (OMNI A1 V10) and two single guide RNAs, that specifically excises a fraction of the mutated allele. Our results demonstrated editing at the site of the SNP in about 80%–90% of the mutant alleles in HSCs from patients harboring a mutation on either the reference or the alternative allele. In contrast, the complementary wild-type allele was maintained intact at about 97%–100%, indicating allele-specific editing took place. NGS analysis of cDNA for the mutation site in excised patient cells showed an enrichment in the wild-type allele compared with non-excised cells, further supporting the knockout of the mutant allele alongside preservation of the wild-type copy. In addition, OMNI A1 V10 showed high fidelity without traceable off targets. These unique features of our nuclease may provide an advantage and should be explored in the context of other indications that are dominant, dominant negative, and compound heterozygous, covering most genetic disorders that other technologies cannot address.

The OMNI A1 V10 composition showed excision efficiency of about 25%. Notably, given the high allele specificity of this nuclease composition, it is estimated that about 50% of the cell population had undergone excision at the mutant allele. With respect to the functional aspects, *ELANE* monoallelic excision significantly enhanced neutrophil differentiation *in vitro*. It also reduced the aberrant numbers of monocytes, consistent with the hematopoietic defect of SCN patients. Excised neutrophils showed normal phagocytic and bacterial killing capacities, indicating that the editing did not impair core neutrophilic functions and is therefore safe. Notably, analysis of phagocytosis out of the total $CD66b^+$ population showed no differences between patient-derived edited and NT neutrophils (Figure S15), supporting the claim that our editing strategy rescues the impaired differentiation arrest in patient-derived cells rather than affecting the function of neutrophils.

In principle, an alternative approach for restoring neutrophil differentiation in SCN-derived HSCs could be templated HDR for correction of *ELANE* mutations.[30] However, in most cases, HDR-based gene correction necessitates tailor-made repair strategies for specific mutations. Given the numerous mutations associated with SCN,[1–4] this approach would be clinically unattainable for some of the patients. In contrast, the editing approach demonstrated in this study is based on targeting SNPs that are frequently heterozygous in the SCN patient population and are linked to the majority of *ELANE* mutations, rather than addressing each mutation independently. Patients' cells were genotyped to determine SNP-mutation linkage. Then, a relevant composition was chosen based on the SNP-mutation localization to either the reference or the alternative allele. By using only three editing strategies (one for each identified SNP, each employing two different compositions directed to either the reference or the alternative allele), the approach described herein could provide a therapeutic solution to more than about 75% of the *ELANE*-mediated SCN patient population through autologous HSC monoallelic editing and subsequent transplantation.

Thus, the current study presents a novel CRISPR-based strategy of specific monoallelic knockout. Such a strategy was found to be efficient, functional, accurate, and safe, thereby providing an alternative therapeutic route for SCN. The technology disclosed herein could potentially offer new therapeutic opportunities for other genetic disorders. Of note, the development of a clinical composition requires additional studies to meet the highest safety and efficacy standards. For example, an *in vivo* engraftment study using an immunocompromised mouse model is needed to support the long-term engraftment and multilineage reconstitution potential of our edited cells.

Moreover, although the GUIDE-seq and *in silico* analyses provided in our study did not depict any off-targets, additional biochemical assays for assessment of off-targets and editing-mediated translocations are necessary.

MATERIALS AND METHODS

Human HSC isolation

HSCs were isolated from SCN patients' bone marrow and healthy donors' mobilized peripheral blood.

Heterozygosity frequency of SNPs in the healthy and patient populations

Variant call files encompassing the *ELANE* gene region (±3 kb of *ELANE*) were downloaded from the 1000 Genomes Project Consortium (phase 3). Genotypes from 2,407 unrelated individuals were analyzed. Three SNPs were chosen (rs3761005, rs1683564, and rs10414837 polymorphisms) to optimize the population coverage for allele-specific *ELANE* knockout. Fifty-three patients' samples were sequenced for the pathogenic mutation and the three chosen SNPs. The heterozygosity frequency of each of the three chosen SNPs and the percentage of the population being heterozygous for at least one of them were calculated for both the healthy and the patient populations.

CRISPR-associated OMNI-A1-V10 ELANE gene editing

An RNP system at a molar ratio of 1:2.5 (OMNI-A1-V10 nuclease:sgRNA) was used. Human $CD34^+$ cells were electroporated using the CA-137 program (Lonza 4D, Nucleofector).

Digital Droplet PCR (excision, allele specificity)

Excision and allele specificity were measured using Digital Droplet PCR on genomic DNA. For excision reaction, amplification of two regions in *ELANE*, exon 1 and exon 5, was performed, using two different probes, FAM(X1) and HEX(X1), respectively. The ratio between the probe signals was translated to excision efficiency. For allele specificity, a FAM probe (binding the alternative allele) and a HEX probe (binding the reference allele) were used (FAM + HEX). The ratio between the two probes was normalized to endogenous genes.

Assessment of mutated:wild-type allele ratio

cDNAs were mapped using NGS targeting exons 4 and 5 harboring S126L and R220Q mutations in patients 41 and 55, respectively. The relative ratio of mutated:wild-type alleles in treated cells was calculated and compared with that of NT cells.

ELANE mRNA expression levels estimate

RNA was purified from day 6 differentiated patient HSCs excised with either RNP(ref) or RNP(alt), mock treated or not treated, using the RNeasy Mini Kit (Qiagen no. 74104). cDNA was prepared using a High-Capacity RNA-to-cDNA kit (Applied Biosystems, no. 4387406). *ELANE* expression levels were measured by ddPCR and normalized to *GAPDH* mRNA levels. Data are presented relative to *ELANE* levels in mock or NT samples.

Differentiation assay

Edited and NT HSCs were subjected to a differentiation protocol adopted from Nasri et al.[19] On day 14, cells were analyzed by flow cytometry for monocytic ($CD14^+/CD66b^-$) and neutrophilic ($CD66b^+$), ($CD11b^+/CD15^+$) subsets.

Bacterial-killing assay

Day 13 differentiated HSCs were evaluated for their bacterial-killing capacity as described in Atosuo and Lilius,[52] using luciferase-expressing bacteria.[53] RLUs were measured over 5 h. The last time point presented is when RLU levels reached plateau. Wells without differentiated HSCs (*E. coli* only) and with the phagocytosis inhibitor cytochalasin D (data not shown) served as controls.

Phagocytosis assay

Phagocytosis capacity was evaluated using the EZCell phagocytosis assay kit (Green Zymosan) (BioVision, cat. no. K397). Cells were analyzed by flow cytometry for internalization of opsonized fluorescent zymosan green particles.

Further details on fluorescence-activated cell sorting (FACS) antibodies, probes, sequences, assays, protocols, and additional methods are provided in the supplemental information.

SUPPLEMENTAL INFORMATION

Supplemental information can be found online at https://doi.org/10.1016/j.omtm.2022.06.002.

ACKNOWLEDGMENTS

This study was supported by research funding from EmendoBio, Inc., and the National Institute of Health (1RO1HL151629 and 5R24AI049393) to D.C.D. and Gil Harari, PhD (CEO, MediStat Ltd), assisted with statistical analysis. The work presented in this article was done in Seattle, Washington, USA.

AUTHOR CONTRIBUTIONS

P.S., V.M., Y.D., A.H., R.E., and D.C.D. designed the research. P.S., Y.D., L.P., D.E., E.S., O.H., and T.P. performed research, analyzed, and interpreted data. L.R., T.B., and M.G. designed the engineered nuclease; M.A. produced the nuclease. P.S., V.M., L.P., E.S., R.E., and D.C.D. commented on the manuscript. A.L.D. collected and interpreted data, performed statistical analysis, and wrote the manuscript.

DECLARATION OF INTERESTS

L.P., L.R., T.B., D.E., E.S., O.H., M.A., A.L.D., A.H., and R.E. are employed by EmendoBio, Inc., which is the owner of the editing technology reported in this research. Y.D. and M.G. are former employees of EmendoBio, Inc. P.S., V.M., and T.P. receive research funding from EmendoBio, Inc. D.C.D. is a consultant and receives honoraria and research funding from EmendoBio, Inc., Amgen, and X4 Pharmaceuticals.

REFERENCES

1. Skokowa, J., Dale, D.C., Touw, I.P., Zeidler, C., and Welte, K. (2017). Severe congenital neutropenias. Nat. Rev. Dis. Primer *3*, 17032. https://doi.org/10.1038/nrdp.2017.32.
2. Dale, D.C., and Link, D.C. (2009). The many causes of severe congenital neutropenia. N. Engl. J. Med. *360*, 3–5. https://doi.org/10.1056/nejmp0806821.
3. Janeway, K.A. (2007). Chapter 118 - neutropenia. In Comprehensive Pediatric Hospital Medicine, L.B. Zaoutis and V.W. Chiang, eds. (Mosby), pp. 738–743.
4. Makaryan, V., Zeidler, C., Bolyard, A.A., Skokowa, J., Rodger, E., Kelley, M.L., Boxer, L.A., Bonilla, M.A., Newburger, P.E., Shimamura, A., et al. (2015). The diversity of mutations and clinical outcomes for ELANE-associated neutropenia. Curr. Opin. Hematol. *22*, 3–11. https://doi.org/10.1097/moh.0000000000000105.
5. Bellanné-Chantelot, C., Clauin, S., Leblanc, T., Cassinat, B., Rodrigues-Lima, F., Beaufils, S., Vaury, C., Barkaoui, M., Fenneteau, O., Maier-Redelsperger, M., et al. (2004). Mutations in the ELA2 gene correlate with more severe expression of neutropenia: a study of 81 patients from the French Neutropenia Register. Blood *103*, 4119–4125. https://doi.org/10.1182/blood-2003-10-3518.
6. Welte, K., Zeidler, C., and Dale, D.C. (2006). Severe congenital neutropenia. Semin. Hematol. *43*, 189–195. https://doi.org/10.1053/j.seminhematol.2006.04.004.
7. Skokowa, J., Germeshausen, M., Zeidler, C., and Welte, K. (2007). Severe congenital neutropenia: inheritance and pathophysiology. Curr. Opin. Hematol. *14*, 21–28. https://doi.org/10.1097/00062752-200701000-00006.
8. Dale, D.C., Person, R.E., Bolyard, A.A., Aprikyan, A.G., Bos, C., Bonilla, M.A., Boxer, L.A., Kannourakis, G., Zeidler, C., Welte, K., et al. (2000). Mutations in the gene encoding neutrophil elastase in congenital and cyclic neutropenia. Blood *96*, 2317–2322. https://doi.org/10.1182/blood.v96.7.2317.
9. Horwitz, M.S., Duan, Z., Korkmaz, B., Lee, H.-H., Mealiffe, M.E., and Salipante, S.J. (2007). Neutrophil elastase in cyclic and severe congenital neutropenia. Blood *109*, 1817–1824. https://doi.org/10.1182/blood-2006-08-019166.
10. Makaryan, V., Kelley, M.L., Fletcher, B., Bolyard, A.A., Aprikyan, A.A., and Dale, D.C. (2017). Elastase inhibitors as potential therapies for ELANE-associated neutropenia. J. Leukoc. Biol. *102*, 1143–1151. https://doi.org/10.1189/jlb.5a1016-445r.
11. Dale, D.C., Bonilla, M.A., Davis, M.W., Nakanishi, A.M., Hammond, W.P., Kurtzberg, J., Wang, W., Jakubowski, A., Winton, E., Lalezari, P., and JAkubowski, A. (1993). A randomized controlled phase III trial of recombinant human granulocyte colony-stimulating factor (Filgrastim) for treatment of severe chronic neutropenia. Blood *81*, 2496–2502. https://doi.org/10.1182/blood.v81.10.2496.bloodjournal81102496.
12. Rosenberg, P.S., Alter, B.P., Bolyard, A.A., Bonilla, M.A., Boxer, L.A., Cham, B., Fier, C., Freedman, M., Kannourakis, G., Kinsey, S., et al. (2006). The incidence of leukemia and mortality from sepsis in patients with severe congenital neutropenia receiving long-term G-CSF therapy. Blood *107*, 4628–4635. https://doi.org/10.1182/blood-2005-11-4370.
13. Rosenberg, P.S., Zeidler, C., Bolyard, A.A., Alter, B.P., Bonilla, M.A., Boxer, L.A., Dror, Y., Kinsey, S., Link, D.C., Newburger, P.E., et al. (2010). Stable long-term risk of leukaemia in patients with severe congenital neutropenia maintained on G-CSF therapy. Br. J. Haematol. *150*, 196–199. https://doi.org/10.1111/j.1365-2141.2010.08216.x.
14. Donadieu, J., Leblanc, T., Bader Meunier, B., Barkaoui, M., Fenneteau, O., Bertrand, Y., Maier-Redelsperger, M., Micheau, M., Stephan, J.L., Phillipe, N., et al.; French Severe Chronic Neutropenia Study Group (2005). Analysis of risk factors for myelodysplasias, leukemias and death from infection among patients with congenital neutropenia. Experience of the French Severe Chronic Neutropenia Study Group. Haematologica *90*, 45–53.
15. Rotulo, G.A., Beaupain, B., Rialland, F., Paillard, C., Nachit, O., Galambrun, C., Gandemer, V., Bertrand, Y., Neven, B., Dore, E., et al. (2020). HSCT may lower leukemia risk in ELANE neutropenia: a before–after study from the French Severe Congenital Neutropenia Registry. Bone Marrow Transplant. *55*, 1614–1622. https://doi.org/10.1038/s41409-020-0800-1.
16. Fioredda, F., Iacobelli, S., van Biezen, A., Gaspar, B., Ancliff, P., Donadieu, J., Aljurf, M., Peters, C., Calvillo, M., Matthes-Martin, S., et al. (2015). Stem cell transplantation in severe congenital neutropenia: an analysis from the European Society for Blood and Marrow Transplantation. Blood *126*, 1885–1892. quiz 1970. https://doi.org/10.1182/blood-2015-02-628859.
17. Zeidler, C., Welte, K., Barak, Y., Barriga, F., Bolyard, A.A., Boxer, L., Cornu, G., Cowan, M.J., Dale, D.C., Flood, T., et al. (2000). Stem cell transplantation in patients with severe congenital neutropenia without evidence of leukemic transformation. Blood *95*, 1195–1198.
18. Rao, S., Brito-Frazao, J., Serbin, A.V., Yao, Q., Luk, K., Wu, Y., Zeng, J., Ren, C., Watkinson, R., Armant, M., et al. (2019). Gene editing ELANE in human hematopoietic stem and progenitor cells reveals disease mechanisms and therapeutic strategies for severe congenital neutropenia. Blood *134*, 3. https://doi.org/10.1182/blood-2019-131073.
19. Nasri, M., Ritter, M., Mir, P., Dannenmann, B., Aghaallaei, N., Amend, D., Makaryan, V., Xu, Y., Fletcher, B., Bernhard, R., et al. (2020). CRISPR/Cas9-mediated ELANE knockout enables neutrophilic maturation of primary hematopoietic stem and progenitor cells and induced pluripotent stem cells of severe congenital neutropenia patients. Haematologica *105*, 598–609. https://doi.org/10.3324/haematol.2019.221804.
20. Rao, S., Yao, Y., Soares de Brito, J., Yao, Q., Shen, A.H., Watkinson, R.E., Kennedy, A.L., Coyne, S., Ren, C., Zeng, J., et al. (2021). Dissecting ELANE neutropenia pathogenicity by human HSC gene editing. Cell Stem Cell *28*, 833–845.e5. e5. https://doi.org/10.1016/j.stem.2020.12.015.
21. Hirche, T.O., Benabid, R., Deslee, G., Gangloff, S., Achilefu, S., Guenounou, M., Lebargy, F., Hancock, R.E., and Belaaouaj, A. (2008). Neutrophil elastase mediates innate host protection against Pseudomonas aeruginosa. J. Immunol. *181*, 4945–4954. Baltim. Md 1950. https://doi.org/10.4049/jimmunol.181.7.4945.
22. Tkalcevic, J., Novelli, M., Phylactides, M., Iredale, J.P., Segal, A.W., and Roes, J. (2000). Impaired immunity and enhanced resistance to endotoxin in the absence of neutrophil elastase and cathepsin G. Immunity *12*, 201–210. https://doi.org/10.1016/s1074-7613(00)80173-9.
23. Belaaouaj, A. (2002). Neutrophil elastase-mediated killing of bacteria: lessons from targeted mutagenesis. Microbes Infect. *4*, 1259–1264. https://doi.org/10.1016/s1286-4579(02)01654-4.
24. Belaaouaj, A., McCarthy, R., Baumann, M., Gao, Z., Ley, T.J., Abraham, S.N., and Shapiro, S.D. (1998). Mice lacking neutrophil elastase reveal impaired host defense against gram negative bacterial sepsis. Nat. Med. *4*, 615–618. https://doi.org/10.1038/nm0598-615.
25. Reeves, E.P., Lu, H., Jacobs, H.L., Messina, C.G.M., Bolsover, S., Gabella, G., Potma, E.O., Warley, A., Roes, J., and Segal, A.W. (2002). Killing activity of neutrophils is mediated through activation of proteases by K+ flux. Nature *416*, 291–297. https://doi.org/10.1038/416291a.
26. Weinrauch, Y., Drujan, D., Shapiro, S.D., Weiss, J., and Zychlinsky, A. (2002). Neutrophil elastase targets virulence factors of enterobacteria. Nature *417*, 91–94. https://doi.org/10.1038/417091a.
27. Benabid, R., Wartelle, J., Malleret, L., Guyot, N., Gangloff, S., Lebargy, F., and Belaaouaj, A. (2012). Neutrophil elastase modulates cytokine expression. J. Biol. Chem. *287*, 34883–34894. https://doi.org/10.1074/jbc.m112.361352.
28. Brinkmann, V., Reichard, U., Goosmann, C., Fauler, B., Uhlemann, Y., Weiss, D.S., Weinrauch, Y., and Zychlinsky, A. (2004). Neutrophil extracellular traps kill bacteria. Science *303*, 1532–1535. https://doi.org/10.1126/science.1092385.
29. Cui, C., Chakraborty, K., Tang, X.A., Zhou, G., Schoenfelt, K.Q., Becker, K.M., Hoffman, A., Chang, Y.-F., Blank, A., Reardon, C.A., et al. (2021). Neutrophil elastase selectively kills cancer cells and attenuates tumorigenesis. Cell *184*, 3163–3177.e21. https://doi.org/10.1016/j.cell.2021.04.016.
30. Tran, N.T., Graf, R., Wulf-Goldenberg, A., Stecklum, M., Strauß, G., Kühn, R., Kocks, C., Rajewsky, K., and Chu, V.T. (2020). CRISPR-Cas9-Mediated ELANE mutation correction in hematopoietic stem and progenitor cells to treat severe congenital neutropenia. Mol. Ther. J. Am. Soc. Gene Ther. *28*, 2621–2634. https://doi.org/10.1016/j.ymthe.2020.08.004.
31. DeWitt, M.A., Magis, W., Bray, N.L., Wang, T., Berman, J.R., Urbinati, F., Heo, S.-J., Mitros, T., Muñoz, D.P., Boffelli, D., et al. (2016). Selection-free genome editing of the sickle mutation in human adult hematopoietic stem/progenitor cells. Sci. Transl. Med. *8*, 360ra134. https://doi.org/10.1126/scitranslmed.aaf9336.
32. Kuo, C.Y., Long, J.D., Campo-Fernandez, B., de Oliveira, S., Cooper, A.R., Romero, Z., Hoban, M.D., Joglekar, A.V., Lill, G.R., Kaufman, M.L., et al. (2018). Site-specific

gene editing of human hematopoietic stem cells for X-linked hyper-IgM syndrome. Cell Rep. *23*, 2606–2616. https://doi.org/10.1016/j.celrep.2018.04.103.

33. Pavel-Dinu, M., Wiebking, V., Dejene, B.T., Srifa, W., Mantri, S., Nicolas, C.E., Lee, C., Bao, G., Kildebeck, E.J., Punjya, N., et al. (2019). Gene correction for SCID-X1 in long-term hematopoietic stem cells. Nat. Commun. *10*, 1634. https://doi.org/10.1038/s41467-019-09614-y.

34. Romero, Z., Lomova, A., Said, S., Miggelbrink, A., Kuo, C.Y., Campo-Fernandez, B., Hoban, M.D., Masiuk, K.E., Clark, D.N., Long, J., et al. (2019). Editing the sickle cell disease mutation in human hematopoietic stem cells: comparison of endonucleases and homologous donor templates. Mol. Ther. *27*, 1389–1406. https://doi.org/10.1016/j.ymthe.2019.05.014.

35. Radtke, S., Pande, D., Cui, M., Perez, A.M., Chan, Y.-Y., Enstrom, M., Schmuck, S., Berger, A., Eunson, T., Adair, J.E., and Kiem, H.P. (2020). Purification of human CD34+CD90+ HSCs reduces target cell population and improves lentiviral transduction for gene therapy. Mol. Ther. - Methods Clin. Dev. *18*, 679–691. https://doi.org/10.1016/j.omtm.2020.07.010.

36. Donini, M., Fontana, S., Savoldi, G., Vermi, W., Tassone, L., Gentili, F., Zenaro, E., Ferrari, D., Notarangelo, L.D., Porta, F., et al. (2007). G-CSF treatment of severe congenital neutropenia reverses neutropenia but does not correct the underlying functional deficiency of the neutrophil in defending against microorganisms. Blood *109*, 4716–4723. https://doi.org/10.1182/blood-2006-09-045427.

37. Horwitz, M.S., Corey, S.J., Grimes, H.L., and Tidwell, T. (2013). ELANE mutations in cyclic and severe congenital neutropenia: genetics and pathophysiology. Hematol. Oncol. Clin. North Am. *27*, 19–41. vii.

38. Germeshausen, M., Deerberg, S., Peter, Y., Reimer, C., Kratz, C.P., and Ballmaier, M. (2013). The spectrum of ELANE mutations and their implications in severe congenital and cyclic neutropenia. Hum. Mutat. *34*, 905–914. https://doi.org/10.1002/humu.22308.

39. Dale, D.C., and Makaryan, V. (1993). ELANE-related Neutropenia. In GeneReviews®, M.P. Adam, H.H. Ardinger, R.A. Pagon, S.E. Wallace, L.J. Bean, G. Mirzaa, and A. Amemiya, eds. (University of Washington, Seattle).

40. Briars, G.L., Parry, H.F., and Ansari, B.M. (1996). Dominantly inherited severe congenital neutropenia. J. Infect. *33*, 123–126. https://doi.org/10.1016/s0163-4453(96)93081-9.

41. Li, F.-Q., and Horwitz, M. (2001). Characterization of mutant neutrophil elastase in severe congenital neutropenia. J. Biol. Chem. *276*, 14230–14241. https://doi.org/10.1074/jbc.m010279200.

42. Aprikyan, A.A.G., Kutyavin, T., Stein, S., Aprikian, P., Rodger, E., Liles, W.C., Boxer, L.A., and Dale, D.C. (2003). Cellular and molecular abnormalities in severe congenital neutropenia predisposing to leukemia. Exp. Hematol. *31*, 372–381. https://doi.org/10.1016/s0301-472x(03)00048-1.

43. Grenda, D.S., Murakami, M., Ghatak, J., Xia, J., Boxer, L.A., Dale, D., Dinauer, M.C., and Link, D.C. (2007). Mutations of the ELA2 gene found in patients with severe congenital neutropenia induce the unfolded protein response and cellular apoptosis. Blood *110*, 4179–4187. https://doi.org/10.1182/blood-2006-11-057299.

44. Köllner, I., Sodeik, B., Schreek, S., Heyn, H., von Neuhoff, N., Germeshausen, M., Zeidler, C., Krüger, M., Schlegelberger, B., Welte, K., and Beger, C. (2006). Mutations in neutrophil elastase causing congenital neutropenia lead to cytoplasmic protein accumulation and induction of the unfolded protein response. Blood *108*, 493–500. https://doi.org/10.1182/blood-2005-11-4689.

45. Nayak, R.C., Trump, L.R., Aronow, B.J., Myers, K., Mehta, P., Kalfa, T., Wellendorf, A.M., Valencia, C.A., Paddison, P.J., Horwitz, M.S., et al. (2015). Pathogenesis of *ELANE*-mutant severe neutropenia revealed by induced pluripotent stem cells. J. Clin. Invest. *125*, 3103–3116. https://doi.org/10.1172/jci80924.

46. Garcia, R., Gusmani, L., Murgia, R., Guarnaccia, C., Cinco, M., and Rottini, G. (1998). Elastase is the only human neutrophil granule protein that alone is responsible for in vitro killing of Borrelia burgdorferi. Infect. Immun. *66*, 1408–1412. https://doi.org/10.1128/iai.66.4.1408-1412.1998.

47. López-Boado, Y.S., Espinola, M., Bahr, S., and Belaaouaj, A. (2004). Neutrophil serine proteinases cleave bacterial Flagellin, abrogating its host response-inducing activity. J. Immunol. *172*, 509–515. https://doi.org/10.4049/jimmunol.172.1.509.

48. Papayannopoulos, V., Metzler, K.D., Hakkim, A., and Zychlinsky, A. (2010). Neutrophil elastase and myeloperoxidase regulate the formation of neutrophil extracellular traps. J. Cell Biol. *191*, 677–691. https://doi.org/10.1083/jcb.201006052.

49. ELANE | gnomAD v2.1.1 | gnomAD. https://gnomad.broadinstitute.org/gene/ENSG00000197561?dataset=gnomad_r2_1.

50. Horwitz, M.S., Laurino, M.Y., and Keel, S.B. (2019). Normal peripheral blood neutrophil numbers accompanying ELANE whole gene deletion mutation. Blood Adv. *3*, 2470–2473. https://doi.org/10.1182/bloodadvances.2019000498.

51. Oikemus, S.R., Pfister, E., Sapp, E., Chase, K.O., Kennington, L.A., Hudgens, E., Miller, R., Zhu, L.J., Chaudhary, A., Mick, E.O., et al. (2021). Allele-specific knockdown of mutant HTT protein via editing at coding region SNP heterozygosities. Hum. Gene Ther.

52. Atosuo, J.T., and Lilius, E.-M. (2011). The real-time-based assessment of the microbial killing by the antimicrobial compounds of neutrophils. Sci. World J. *11*, 2382–2390. https://doi.org/10.1100/2011/376278.

53. Karsi, A., and Lawrence, M.L. (2007). Broad host range fluorescence and bioluminescence expression vectors for Gram-negative bacteria. Plasmid *57*, 286–295. https://doi.org/10.1016/j.plasmid.2006.11.002.

OMTM, Volume *26*

Supplemental information

Mutant allele knockout with novel CRISPR nuclease promotes myelopoiesis in ELANE neutropenia

Peter Sabo, Vahagn Makaryan, Yosef Dicken, Lital Povodovski, Liat Rockah, Tzlil Bar, Matan Gabay, Dalia Elinger, Ella Segal, Ora Haimov, Maya Antoshvili, Anat London Drori, Tanoya Poulsen, Asael Herman, Rafi Emmanuel, and David C. Dale

Supplemental Information

Supplemental Figures

Figure S1.

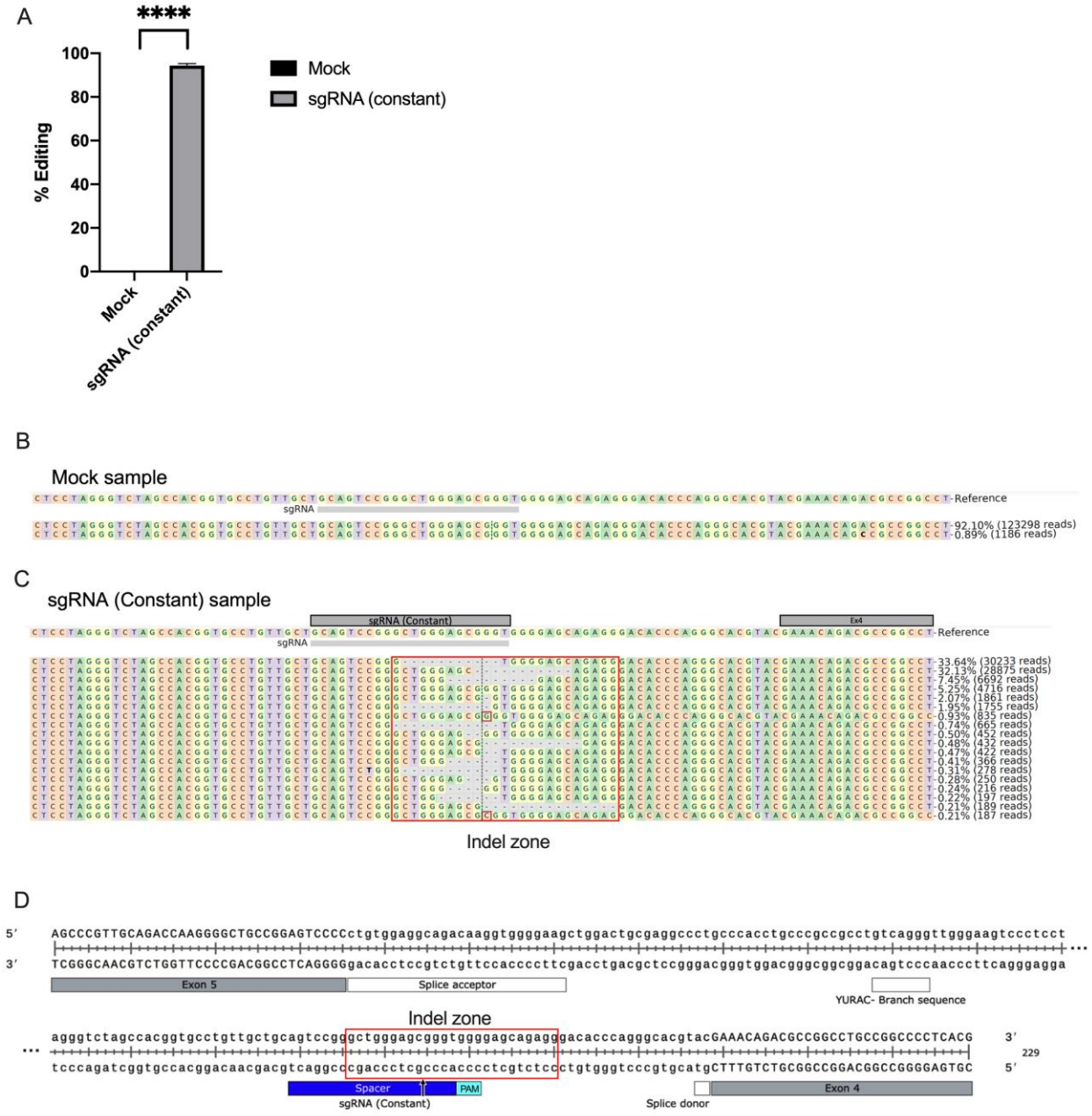

Figure S1. Editing by sgRNA (constant). (A) Bar graphs representing percentages of editing in HSCs taken from a healthy donor that were either electroporated without nuclease and guides (Mock, black) or treated with OMNI-A1 V10 nuclease and only sgRNA (constant) (sgRNA (constant), gray) as measured by ddPCR. (n=3 groups of cells). Statistical significance is indicated as ****P<.0001. Bars represent mean values with standard deviation. (B and C) NGS outputs of Mock-treated (Mock sample, B) and sgRNA (constant)-treated cells (C). The area where indels were detected is lineated by a red square (Indel zone). sgRNA (constant) and exon 4 (EX4) locations are depicted in gray. Only reads above 0.2% are presented. (D) Schematic of a section of *ELANE* gene (spanning from exon 5 in the upper row to exon 4 in the lower row) depicting exon 4, exon 5, sgRNA(constant) and regulatory elements: Splice

acceptor, branch sequence and splice donor. The area where indels were detected following editing with sgRNA(constant) is lineated by a red square (Indel zone).

Figure S2.

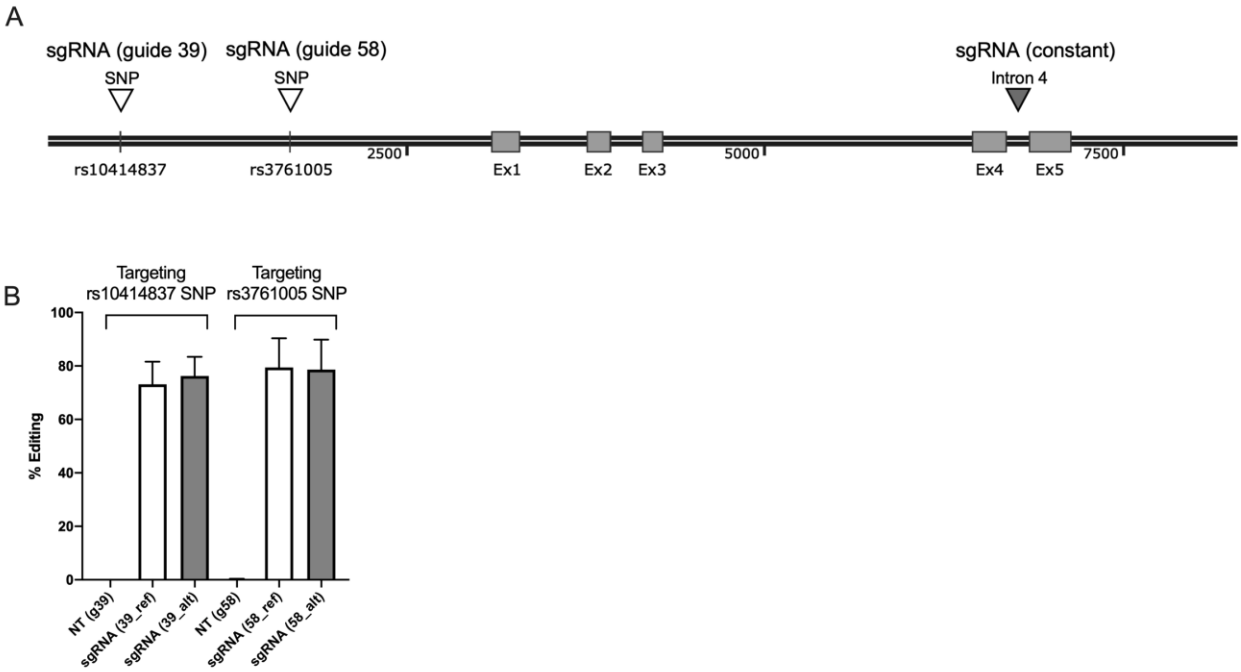

Figure S2. Targeting upstream SNPs. (A) Schematic of ELANE gene depicting rs10414837 and rs3761005 SNPs and their corresponding sgRNAs, guides 39 and 58, respectively. (B) Bar graphs representing percentages of editing in U2OS cells that were either not-treated (NT, black) or electroporated with the non-engineered nuclease, OMNI-A1, and sgRNA 39 or sgRNA 58 targeting the reference (white) or alternative (gray) forms of the SNPs as measured by ddPCR. (n=3 groups of cells). Bars represent mean values with standard deviation.

Figure S3.

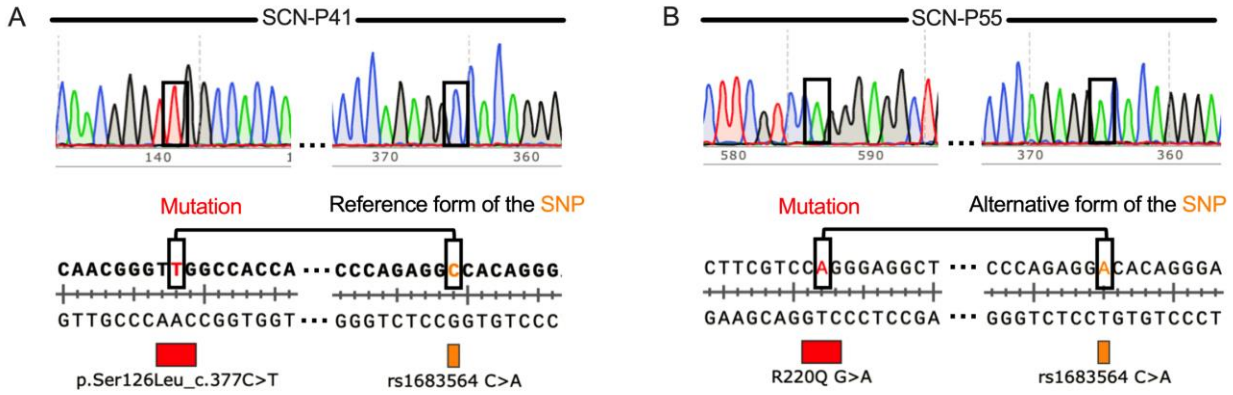

Figure S3. Mutation-SNP linkage determination in SCN-P41 and SCN-P55 patients. Electropherograms of sequencing analyses of the mutation site and the rs1683564 SNP. (A) SCN-P41 patient harbors a mutation (red) on the same allele as the reference form of the SNP (C, cytosine, orange), whereas (B) SCN-P55 patient harbors a mutation (red) on the same allele as the alternative form of the SNP (A, adenosine, orange).

Figure S4.

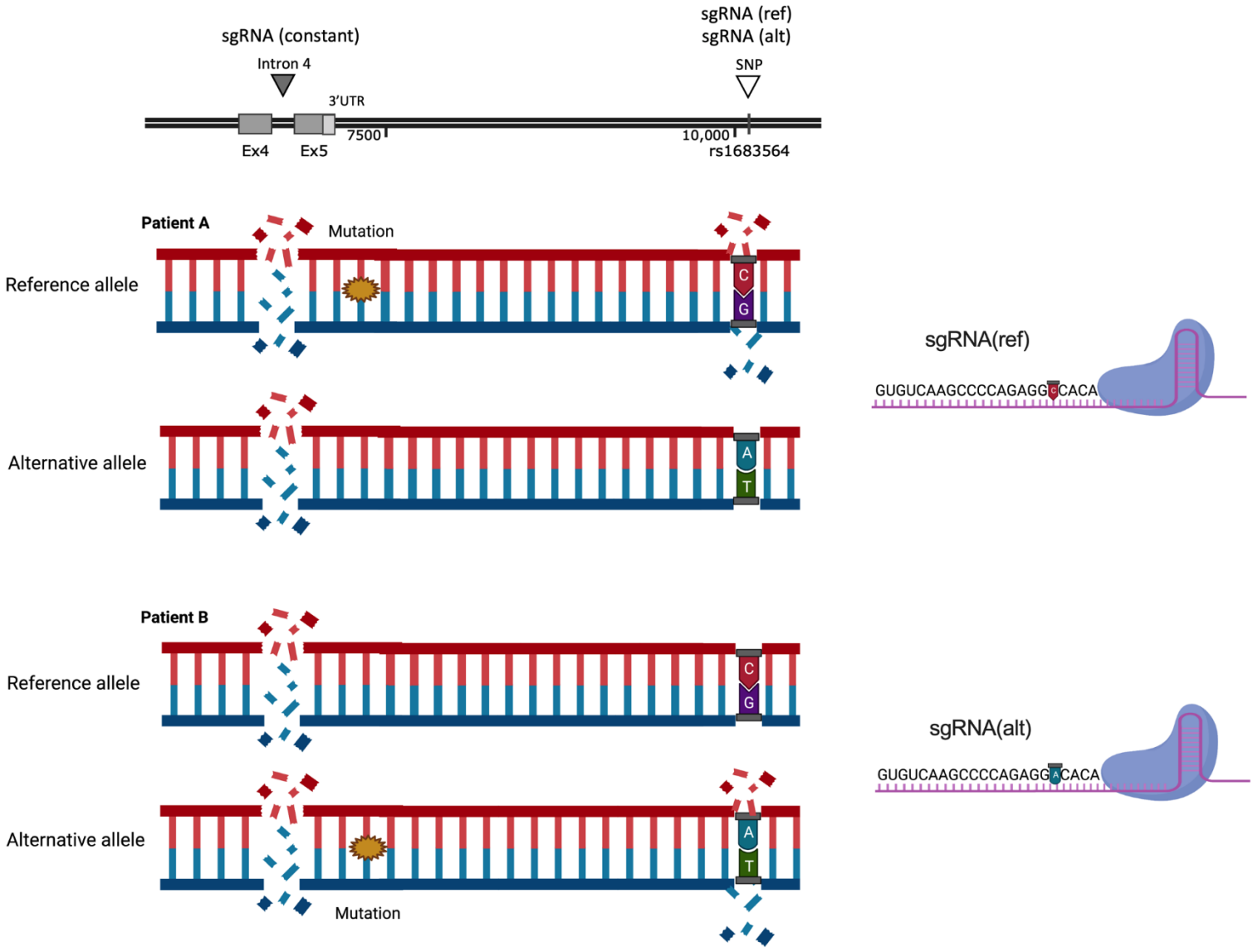

Figure S4. Same editing outcomes with RNP(ref) and RNP(alt) compositions. The *ELANE* gene is cleaved in two locations: 1) intron 4, a biallelic site guided by sgRNA(constant) guide and 2) a heterozygous SNP site, rs1683564, a single allelic site guided by either sgRNA(ref) or sgRNA(alt) depending on the linkage to the mutation site. If the mutation is located at the allele harboring the reference form of the SNP (C, cytosine), RNP(ref) composition, including a nuclease, sgRNA(ref) and sgRNA(constant), is chosen and a section of the reference mutated allele is cleaved (Patient A, upper panel). If the mutation is located at the allele harboring the alternative form of the SNP (A, adenosine), RNP(alt) composition, including a nuclease, sgRNA(alt) and sgRNA(constant), is chosen and a section of the alternative mutated allele is cleaved (Patient B, lower panel). Illustration created with BioRender.com.

Figure S5.

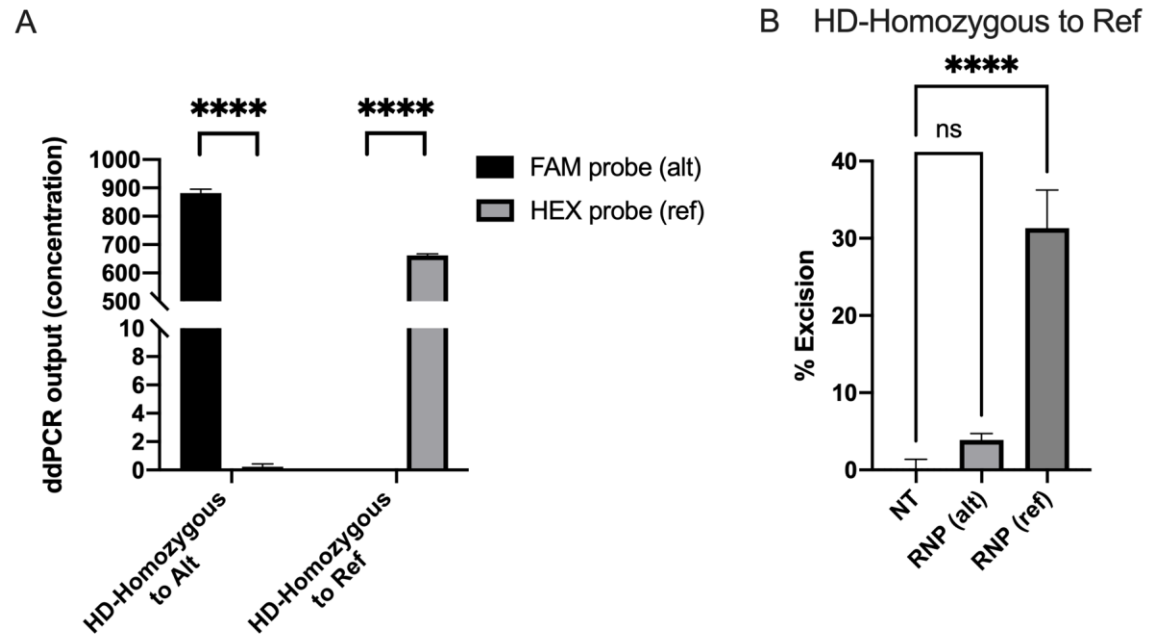

Figure S5. Probes' and guides' specificity. (A) The binding of each probe (FAM, black; HEX, gray) to DNA extracted from healthy donor (HD) cells that are homozygous to either the reference or alternative forms of the SNP, was measured by ddPCR. Bar graphs representing concentration of positive events. (n=3 groups of cells). Statistical significance is indicated as ****P<.0001. (B) Bar graphs representing percentages of excision in a healthy donor HSCs that are homozygous to the reference form of the rs1683564 SNP and were either not-treated (NT), treated with RNP(alt) or RNP(ref) as measured by ddPCR. (n=3 groups of cells). Statistical significance is indicated as ****P<.0001, ns = Not statistically significant. Bars represent mean values with standard deviation.

Figure S6.

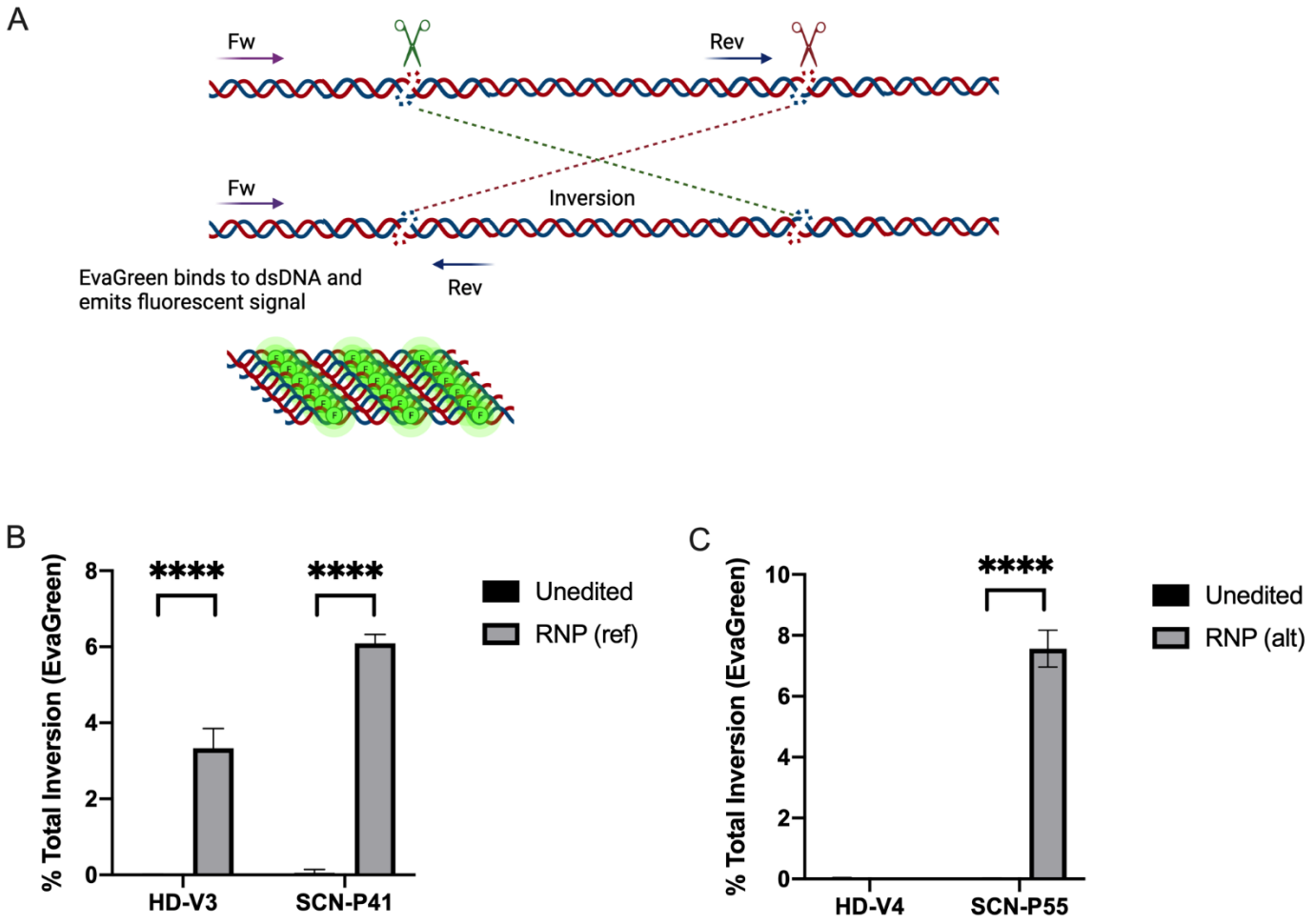

Figure S6. Inversion events following excision. (A) Schematic of detection of inversion events: Specific primers were designed to amplify inverted variations of the excised fragment. EvaGreen dye, a fluorescent DNA-binding dye that binds dsDNA, was used in a ddPCR assay to measure all inversion events. Illustration created with BioRender.com. (B) Quantification of total inversion events measured by EvaGreen-based ddPCR assay in unedited (black) and RNP(ref)-treated (gray) HD-V3 healthy donor and SCN-P41 patient derived differentiated HSCs. Statistical significance is indicated as ****P<.0001. (C) Quantification of total inversion events measured by EvaGreen-based ddPCR assay in unedited HD-V4 healthy donor and SCN-P55 patient-derived differentiated HSCs (black) and in RNP(alt)-treated (gray) SCN-P55 patient-derived differentiated HSCs. Statistical significance is indicated as ****P<.0001. Bars represent mean values with standard deviation. (n=3-4 groups of cells from HD-V3 or HD-V4 healthy /SCN-P41 or SCN-P55 patient donors).

Figure S7.

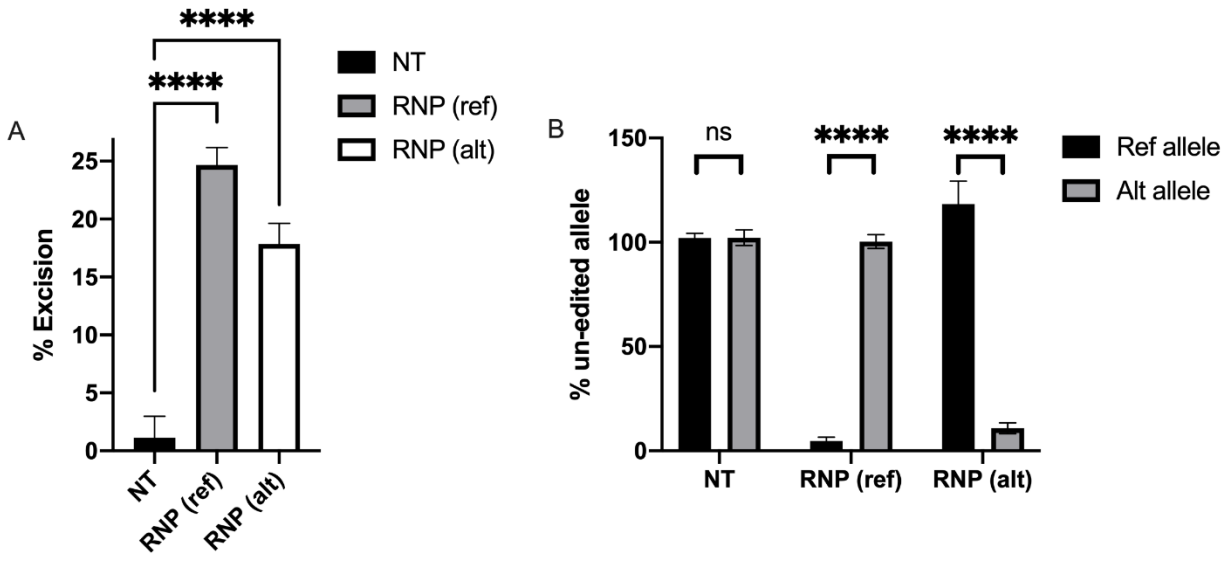

Figure S7. Excision levels and allele specificity in additional healthy donors. (A) Bar graphs representing percentages of excision in HSCs taken from healthy donors that were either non-treated (NT, black), RNP (ref)-treated (gray) or RNP(alt)-treated (white) as measured by ddPCR. (n=4 groups of cells from 2 healthy donors in each group). Statistical significance is indicated as ****P<.0001. (B) Bar graphs representing percentages of un-edited reference (black) and alternative (gray) alleles in HSCs taken from healthy donors that were non-treated (NT), treated with RNP(ref) or RNP(alt), as measured by ddPCR. Average of each allele concentration was normalized to endogenous gene control RPP30 and STAT1 and presented relatively to non-treated cells. (n=4 groups of cells from 2 healthy donors in each group). Statistical significance is indicated as ****P<.0001, ns = Not statistically significant. Bars represent mean values with standard deviation.

Figure S8.

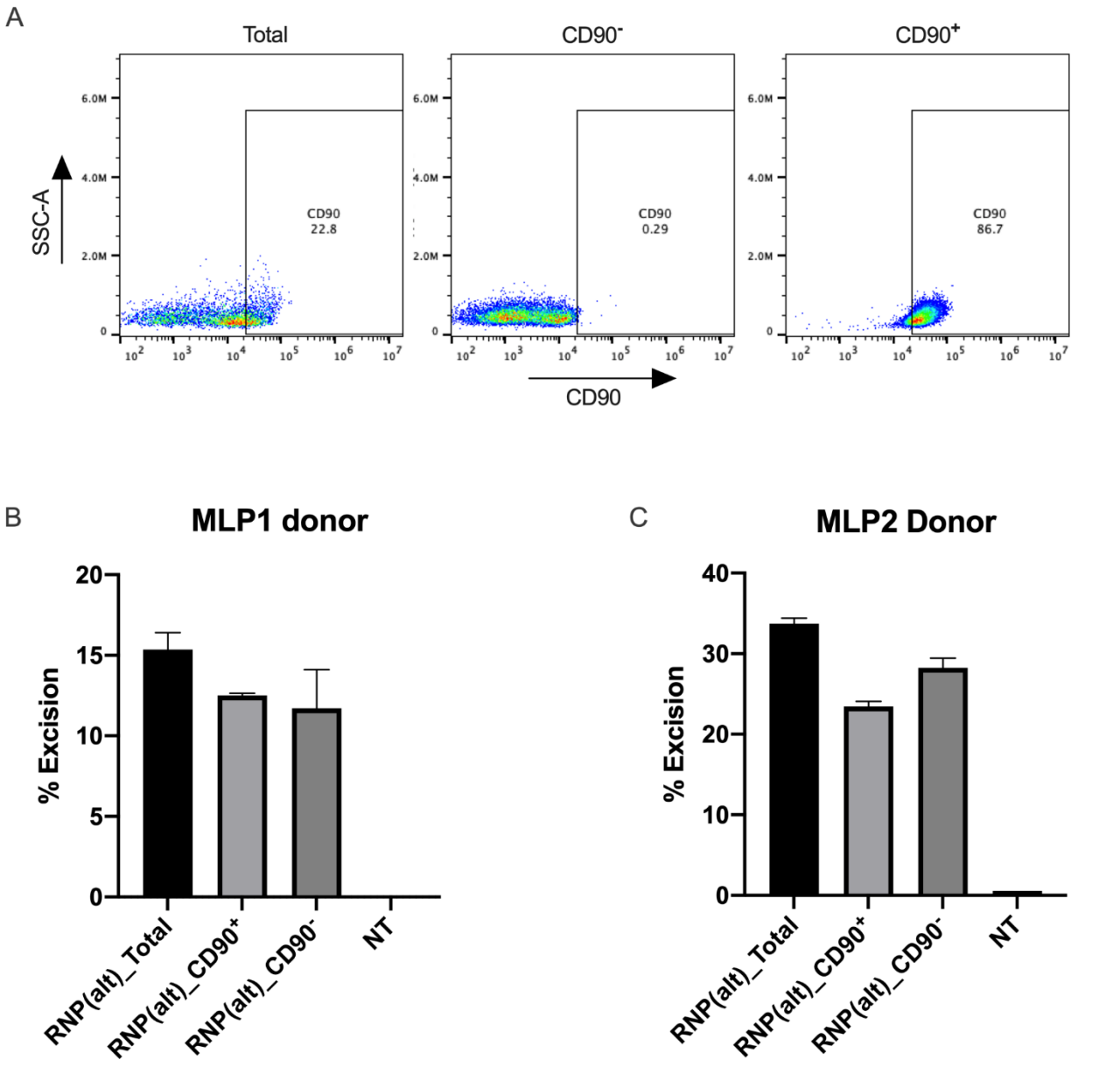

Figure S8. Excision levels in Long Term HSC population. (A) Representative FACS plots of healthy donor-derived $CD34^+$ HSCs prior to sorting (Total, left panel) and following sorting to $CD90^-$ (middle panel) and $CD90^+$ (right panel) populations. (B and C) Bar graphs representing percentages of excision from HSCs taken from two healthy donors (MLP1; B - heterozygous to the alternative form of the SNP and MLP2, C - homozygous to the alternative form of the SNP) prior to sorting (Total, black) and following sorting to $CD90^+$ (light gray) and $CD90^-$ (dark gray) populations as measured by ddPCR. Non-treated HSCs prior to sorting served as control (NT) (n=2 groups of cells from each healthy donor in each group). Bars represent mean values with standard deviation.

Figure S9.

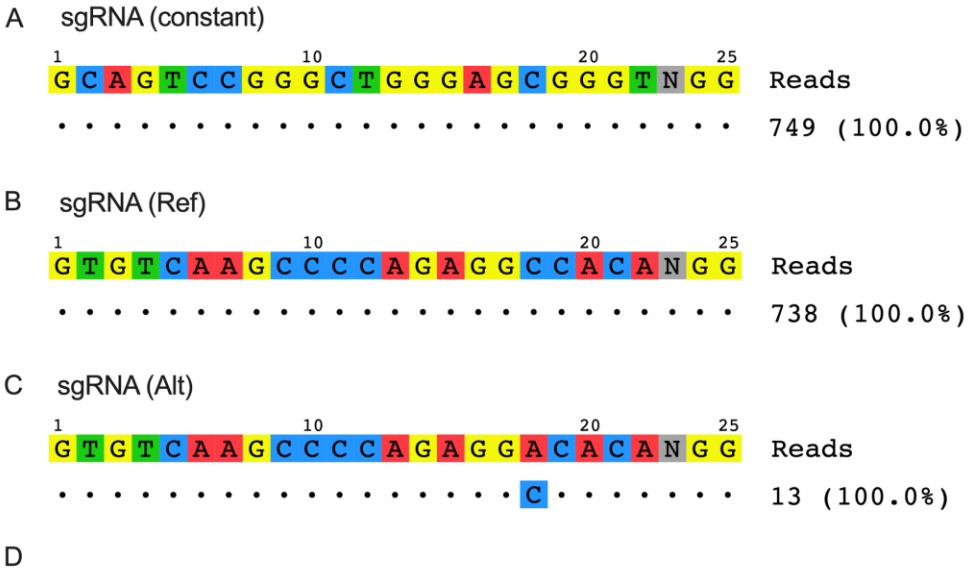

D

Chromosome	Position	Gene	Type	Sequence	Mismatches	Reads SCN-P41	Reads SCN-P55
sgRNA-Int4-const							
chr15	90957975	RCCD1	intron	aCAGTCCtGGCTGGGAGCaGGTGGG	3	0	0.03±0
chr17	74081352	LINC02074	intron	aCAGTCCGGGCTGGGAGCtGGgAGG	3	0	0.03±0
sgRNA-564DS-alt							
chr22	28908576	ZNRF3	intron	GTGaCAtGCCCCAtAGGACACAGGG	3		0
chr2	26950233	DPYSL5	exon	GTGTCAAcCCCaAGAcGACACATGG	3		0.01±0.01
sgRNA-564DS-ref							
chr12	58121865	NA	intergenic	GTGTgAAGgCCCAGAGGCCAaAGGG	3	0.07±0.02	
chr12	116915161	FBXW8	intron	GTtgCAAGCCCCAGAGcCCACAGGG	3	0.03±0.03	

Figure S9. No detected off targets following editing of OMNI-A1 V10 nuclease and each of the sgRNAs. (A-C) An unbiased survey (GUIDE-seq) of whole-genome off-target cleavage using OMNI A1 V10 nuclease and each of the constant guide (A, SgRNA(constant)), reference guide (B, SgRNA(ref)) and alternative guide (C, SgRNA(alt)), showing all reads are of the target sequence and no off targets detected (≤4 mismatches) (for raw data see Table S2). Note, analysis was done in U2OS cells that are homozygous to the reference form of rs1683564 SNP. Since OMNI-A1 V10 nuclease is highly allele discriminatory, when using sgRNA(alt) there is only minor on-target editing of the reference allele (13 reads of the reference cytosine genotype) and no detectable off targets. (D) A table summarizing the results of an *in-silico* off target analysis for constant, alternative and reference guides depicting a few potential off-targets. None of these off targets were validated by rhAmpSeq analysis performed on HSCs derived from SCN-P41 and SCN-P55 patients edited with RNP(ref) and RNP(alt), respectively, see two right columns. rhAmpSeq validation threshold was set to editing ≥0.2%.

Figure S10.

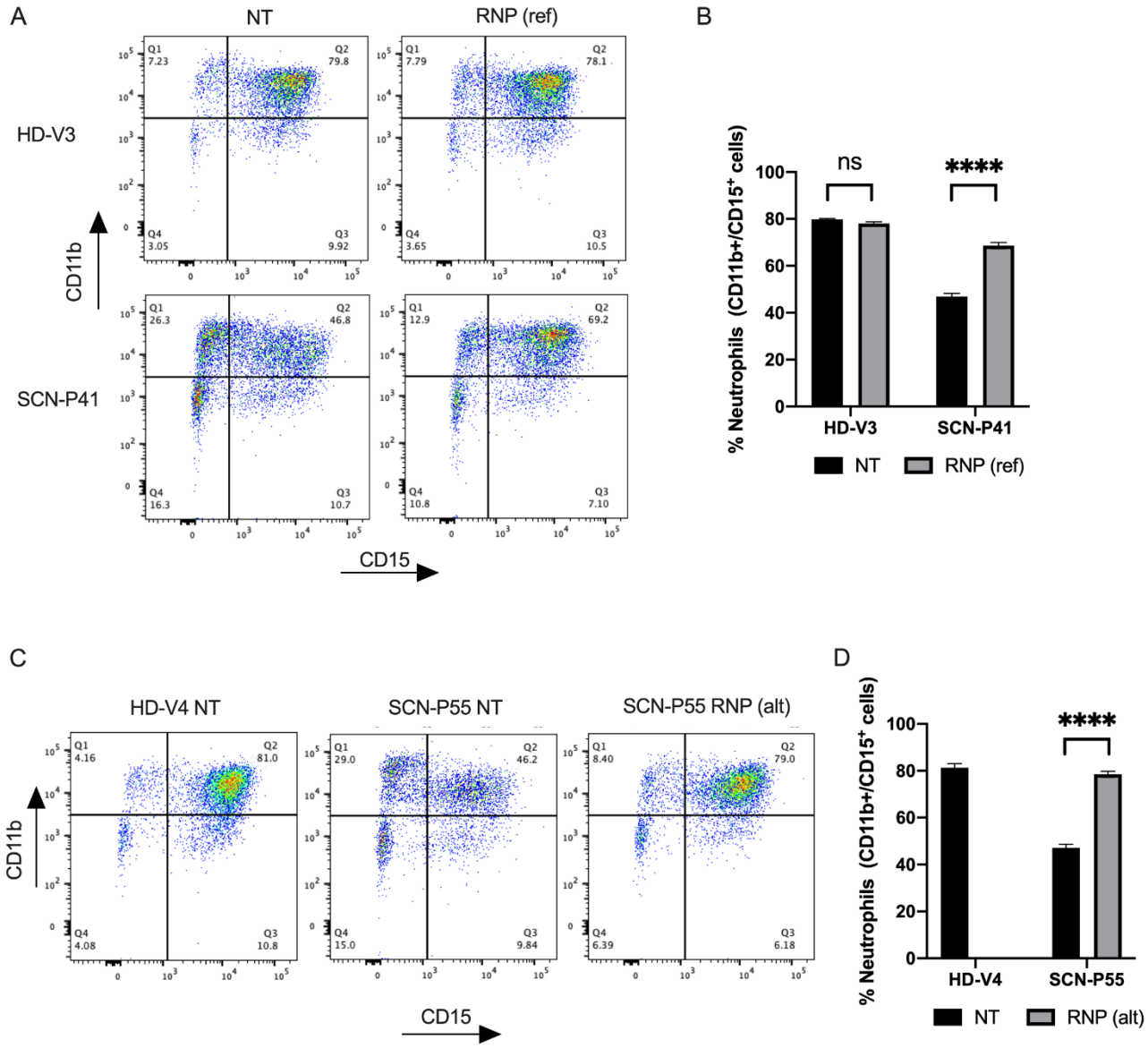

Figure S10. Differentiation into $CD11b^{+}/CD15^{+}$ neutrophils. (A) Representative FACS plots of non-treated (NT, left panel) and RNP(ref)-treated (right panel) healthy donor (HD-V3, upper panel) and SCN-P41 patient (lower panel) differentiated HSCs, analyzed for neutrophilic ($CD11b^{+}/CD15^{+}$) subset. (B) Quantitative analysis of respective FACS data for percentages of neutrophils ($CD11b^{+}/CD15^{+}$ cells) in healthy (HD-V3) and SCN patient (SCN-P41) differentiated HSCs that were non-treated (NT, black) or treated with RNP(ref) (gray). (n=3 groups of cells from HD-V3 healthy /SCN-P41 patient donors). Statistical significance is indicated as ****P<.0001, ns = Not statistically significant. (C) Representative FACS plots of non-treated healthy donor (HD-V4 NT, left panel), non-treated SCN patient (SCN-P55 NT, middle panel) and RNP(alt)-treated SCN patient (right panel) differentiated HSCs, analyzed for neutrophilic ($CD11b^{+}/CD15^{+}$) subset. (D) Quantitative analysis of respective FACS data for percentages of neutrophils ($CD11b^{+}/CD15^{+}$ cells) in differentiated HSCs from non-treated healthy donor (HD-V4, NT; black) and SCN patient (SCN-P55) either non-treated (NT, black) or treated with RNP(alt) (gray). (n=3 groups of cells from HD-V4 healthy /SCN-P55 patient donors). Statistical significance is indicated as ****P<.0001. Bars represent mean values with standard deviation.

Figure S11.

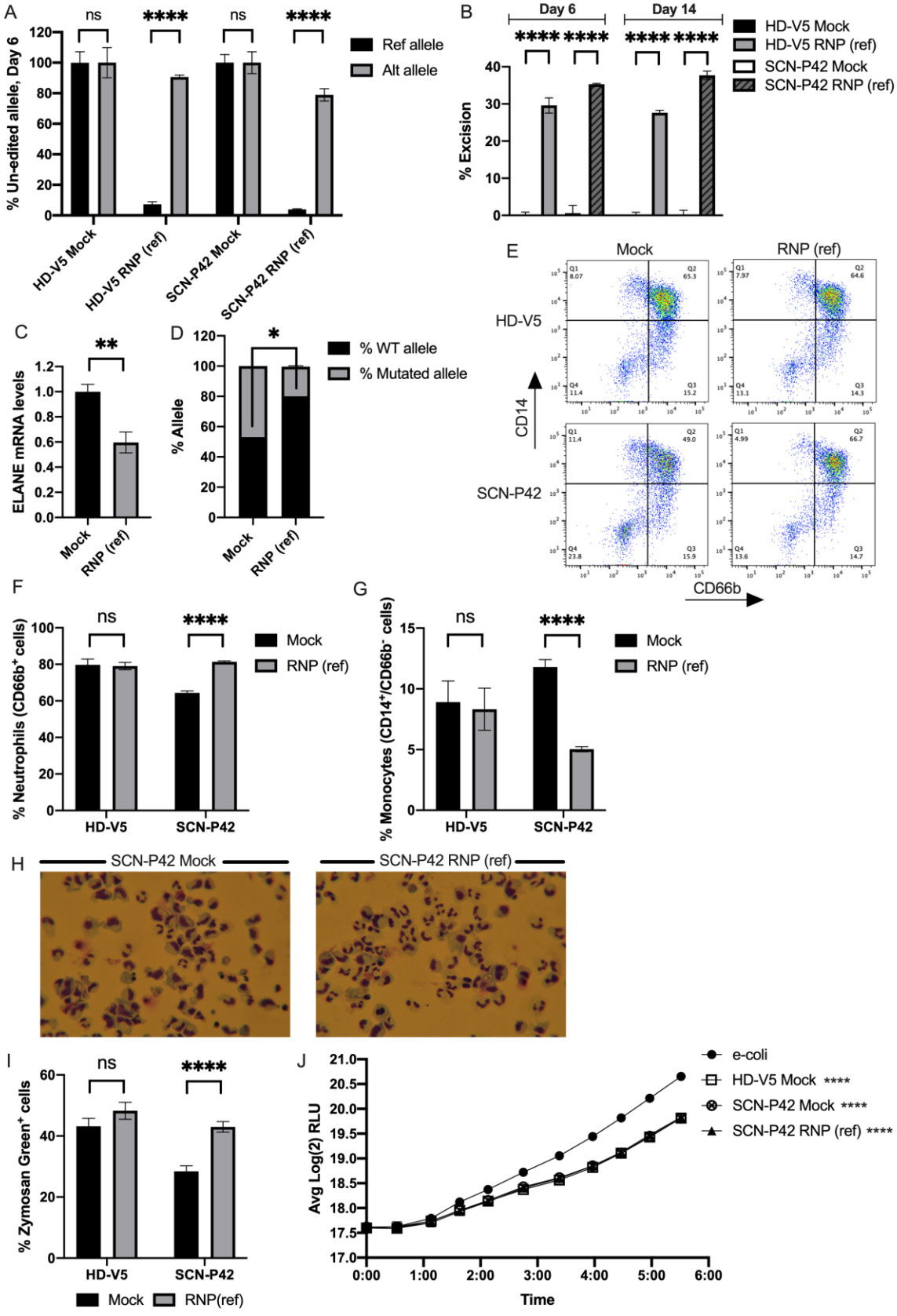
A
ns
****
ns
****
% Un-edited allele, Day 6
Ref allele
Alt allele
HD-V5 Mock
HD-V5 RNP (ref)
SCN-P42 Mock
SCN-P42 RNP (ref)
B
Day 6
Day 14
**** **** **** ****
% Excision
HD-V5 Mock
HD-V5 RNP (ref)
SCN-P42 Mock
SCN-P42 RNP (ref)
C
**
ELANE mRNA levels
Mock
RNP (ref)
D
*
% Allele
% WT allele
% Mutated allele
Mock
RNP (ref)
E
Mock
RNP (ref)
HD-V5
SCN-P42
CD14
CD66b
F
ns
****
% Neutrophils (CD66b+ cells)
Mock
RNP (ref)
HD-V5
SCN-P42
G
ns
****
% Monocytes (CD14+/CD66b- cells)
Mock
RNP (ref)
HD-V5
SCN-P42
H
SCN-P42 Mock
SCN-P42 RNP (ref)
I
ns
****
% Zymosan Green+ cells
HD-V5
SCN-P42
Mock
RNP(ref)
J
Avg Log(2) RLU
Time
e-coli
HD-V5 Mock ****
SCN-P42 Mock ****
SCN-P42 RNP (ref) ****

Figure S11. Excision using RNP(ref) in SCN-P42 and HD-V5. (A) Bar graphs representing percentages of un-edited reference (black) and alternative (gray) alleles at day 6 of differentiation in HSCs taken from either healthy donor (HD-V5) or SCN patient (SCN-P42) treated with RNP (ref) composition or electroporated without a nuclease composition (Mock), as measured by ddPCR. (n=3 groups of cells from HD-V5 healthy/SCN-P42 patient donors). Statistical significance is indicated as ****P<.0001, ns = Not statistically significant. (B) Bar graphs representing percentages of excision at days 6 and 14 of differentiation in HSCs taken from either healthy donor (HD-V5): Mock-treated (Mock, black) or RNP (ref)-treated (gray), or SCN patient (SCN-P42): Mock-treated (Mock, white) or RNP (ref)-treated (dark oblique lines), as measured by ddPCR. (n=3 groups of cells from HD-V5 healthy /SCN-P42 patient donors). Statistical significance is indicated as ****P<.0001. (C) Bar graphs representing *ELANE* mRNA levels in day 6 differentiated HSCs of SCN-P42 patient that were either Mock-treated (Black) or RNP(ref)-treated (Gray). Data is presented relatively to the mock group. (n=3 groups of cells from SCN-P42 patient). Statistical significance is indicated as **P<.01. (D) Bar graphs representing percentages of wild-type (black) and mutated (gray) alleles in cDNA taken from SCN-P42 patient HSCs that were either RNP (ref)-treated or Mock-treated (Mock), as measured by NGS targeting the mutation site. (n=3 groups of cells from SCN-P42 patient). Statistical significance is indicated as *P<.05. (E) Representative FACS plots of mock-treated (Mock, left panel) and RNP(ref)-treated (right panel) healthy donor (HD-V5, upper panel) and SCN-P42 patient (lower panel) differentiated HSCs, analyzed for neutrophilic ($CD66b^+$) and monocytic ($CD14^+/CD66b^-$) subsets. (F) Quantitative analysis of respective FACS data for percentages of neutrophils ($CD66b^+$ cells) in healthy (HD-V5) and SCN patient (SCN-P42) differentiated HSCs that were mock-treated (Mock, black) or treated with RNP(ref) (gray). (n=3 groups of cells from HD-V5 healthy /SCN-P42 patient donors). Statistical significance is indicated as ****P<.0001, ns = Not statistically significant. (G) Quantitative analysis of respective FACS data for percentages of monocytes ($CD14^+/CD66b^-$ cells) in healthy (HD-V5) and SCN patient (SCN-P42) differentiated HSCs that were mock-treated (Mock, black) or treated with RNP(ref) (gray). (n=3 groups of cells from HD-V5 healthy /SCN-P42 patient donors). Statistical significance is indicated as ****P<.0001, ns = Not statistically significant. (H) Diff-Quik staining of P42 SCN patient-derived differentiated HSCs treated with RNP(ref) or electroporated without a nuclease composition (SCN-P42 Mock). Microphotographs were taken on LEITZ LABORLUX S polarizing light microscope at 400X magnification using Nikon DSLR digital camera. (I) Quantification of percentages of Zymosan Green uptake by healthy (HD-V5) and SCN patient (SCN-P42) differentiated HSCs that were mock-treated (Mock, black) or treated with RNP(ref) (gray). Statistical significance is indicated as ****P<.0001, ns = Not statistically significant. (J) Graph depicts real time change in light emission, relative light units (RLUs), from 200,000 Luciferase expressing bacterial cells incubated with differentiated neutrophils from healthy mock-treated (HD-V5, Mock; white square), patient mock-treated (SCN-42 Mock; crossed circle) or patient RNP(ref)-treated (SCN-P42 RNP(ref); triangle) HSCs compared to bacterial cells only control (e-coli, circle). Statistical significance for each one of the groups versus e-coli control at the last time point presented, when RLU levels reached plateau, is indicated as ****P<.0001. Bars represent mean values with standard deviation.

Figure S12.

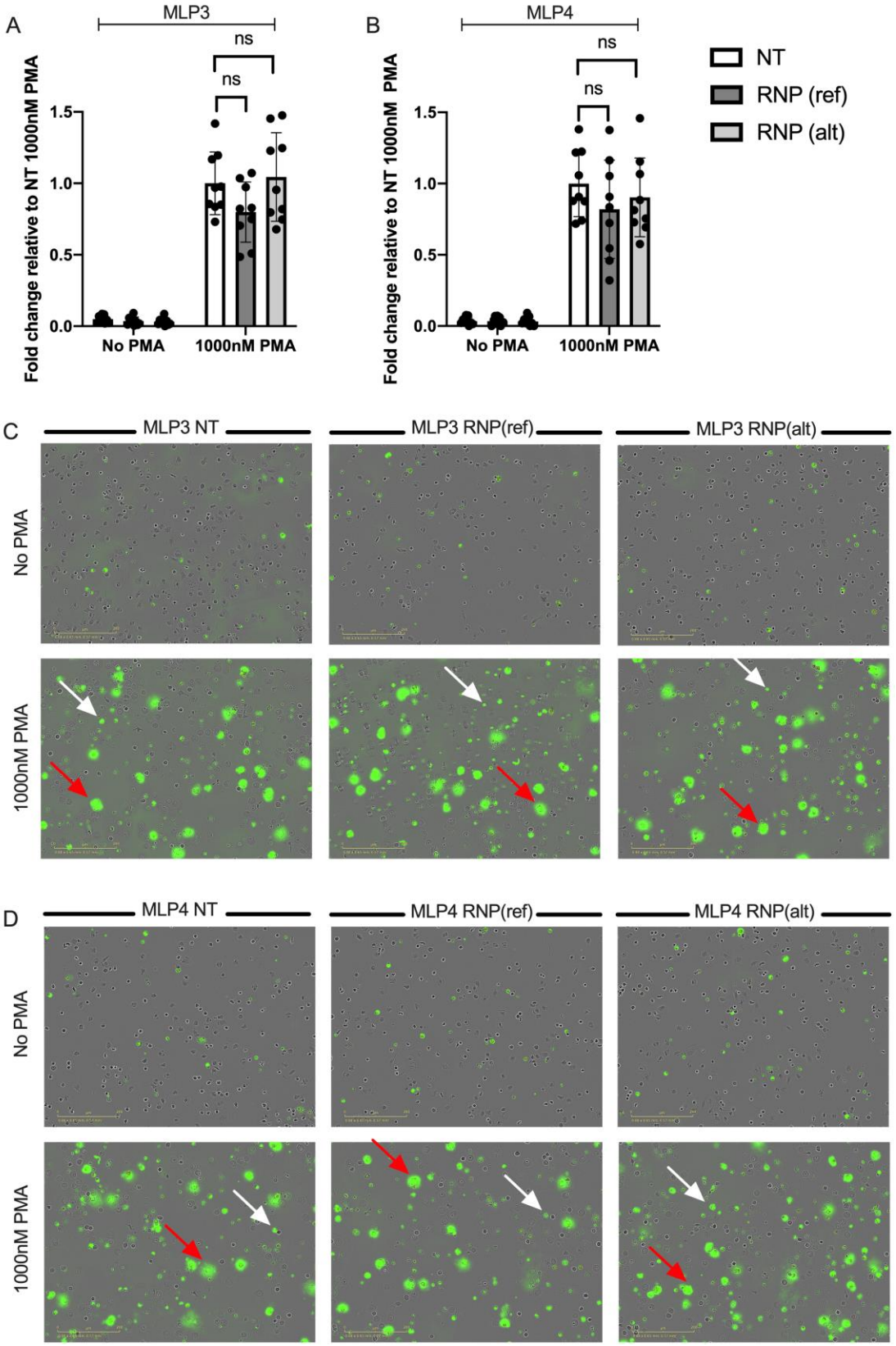
A
MLP3
ns
ns
Fold change relative to NT 1000nM PMA
1.5
1.0
0.5
0.0
No PMA
1000nM PMA
B
MLP4
ns
ns
Fold change relative to NT 1000nM PMA
1.5
1.0
0.5
0.0
No PMA
1000nM PMA
NT
RNP (ref)
RNP (alt)
C
MLP3 NT
MLP3 RNP(ref)
MLP3 RNP(alt)
No PMA
1000nM PMA
D
MLP4 NT
MLP4 RNP(ref)
MLP4 RNP(alt)
No PMA
1000nM PMA

Figure S12. Excision did not compromise NETosis capacity. (A and B) Bar graphs representing fold of change in NETosis levels in differentiated HSCs taken from healthy donors (MLP3 (A) and MLP4 (B)). HSCs were either not-treated (NT), RNP(ref)-treated or RNP(alt)-treated and were stimulated, following differentiation, with PMA (1000nM PMA) or added with 0.1% DMSO (No PMA control) for 10 hours. Cells were incubated with SYTOX Green dye for detection of membrane-damaged cells and imaged by Incucyte® S3 System. Data is presented relatively to averaged NT 1000nM PMA group. (n=9 wells of cells for each condition from 3 independent experiments). Statistical significance is indicated as ns = Not statistically significant. (C and D) Incucyte® images of differentiated HSCs from donors MLP3 (C) and MLP4 (D) that were either not-treated (NT, left panel), RNP(ref)-treated (middle panel) or RNP(alt)-treated (right panel) and were added with 0.1% DMSO (No PMA) or stimulated with PMA (1000nM PMA) in the presence of SYTOX Green dye. Enlarged green cells represent cells undergoing NETosis. Images were acquired with a scale bar of 200 μm. Red and white arrows depict representative NETotic and apoptotic cells, respectively.

Figure S13.

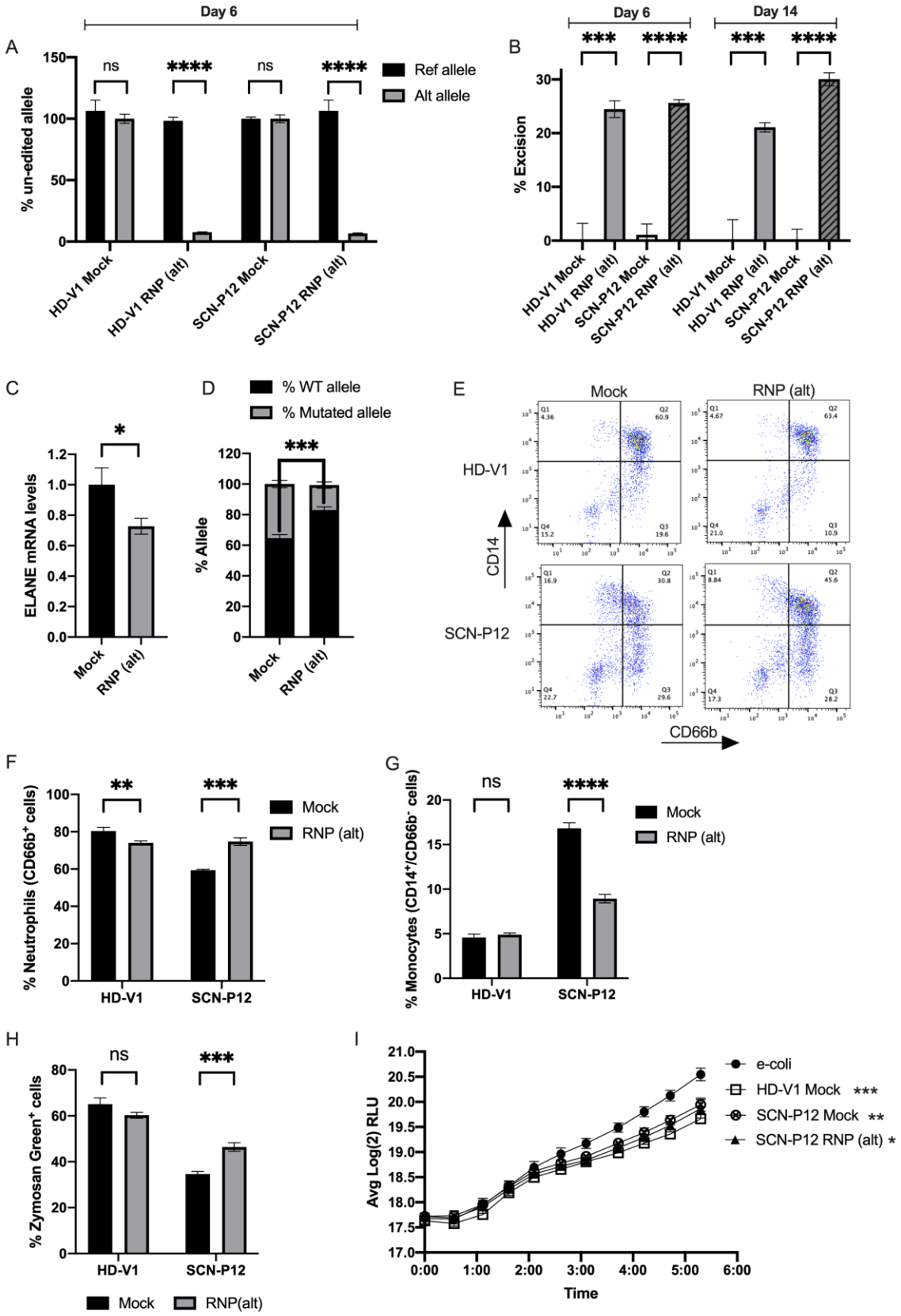
A
Day 6
% un-edited allele
Ref allele
Alt allele
ns
****
ns
****
HD-V1 Mock
HD-V1 RNP (alt)
SCN-P12 Mock
SCN-P12 RNP (alt)
B
Day 6
Day 14
***
****
***
****
% Excision
C
*
ELANE mRNA levels
D
% WT allele
% Mutated allele
***
% Allele
E
Mock
RNP (alt)
HD-V1
SCN-P12
CD14
CD66b
F
**
***
Mock
RNP (alt)
% Neutrophils (CD66b+ cells)
HD-V1
SCN-P12
G
ns
****
% Monocytes (CD14+/CD66b- cells)
H
ns
***
% Zymosan Green+ cells
I
e-coli
HD-V1 Mock ***
SCN-P12 Mock **
SCN-P12 RNP (alt) *
Avg Log(2) RLU
Time

Figure S13. Excision using RNP(alt) in SCN-P12 and HD-V1. (A) Bar graphs representing percentages of un-edited reference (black) and alternative (gray) alleles at day 6 of differentiation in HSCs taken from either healthy donor (HD-V1) or SCN patient (SCN-P12) treated with RNP (alt) composition or electroporated without a nuclease composition (Mock), as measured by ddPCR. (n=3 groups of cells from HD-V1 healthy/SCN-P12 patient donors). Statistical significance is indicated as ****P<.0001, ns = Not statistically significant. (B) Bar graphs representing percentages of excision at days 6 and 14 of differentiation in HSCs taken from either healthy donor (HD-V1): Mock-treated (Mock, black) or RNP (alt)-treated (gray), or SCN patient (SCN-P12): Mock-treated (Mock, white) or RNP (alt)-treated (dark oblique lines), as measured by ddPCR. (n=3 groups of cells from HD-V1 healthy /SCN-P12 patient donors). Statistical significance is indicated as ***P<.001, ****P<.0001. (C) Bar graphs representing *ELANE* mRNA levels in day 6 differentiated HSCs of SCN-P12 patient that were either Mock-treated (Black) or RNP(alt)-treated (Gray). Data is presented relatively to the mock group. (n=3 groups of cells from SCN-P12 patient). Statistical significance is indicated as *P<.05. (D) Bar graphs representing percentages of wild-type (black) and mutated (gray) alleles in cDNA taken from SCN-P12 patient HSCs that were either RNP (alt)-treated or Mock-treated (Mock), as measured by NGS targeting the mutation site. (n=3 groups of cells from SCN-P12 patient). Statistical significance is indicated as ***P<.001. (E) Representative FACS plots of mock-treated (Mock, left panel) and RNP(alt)-treated (right panel) healthy donor (HD-V1, upper panel) and SCN-P12 patient (lower panel) differentiated HSCs, analyzed for neutrophilic ($CD66b^+$) and monocytic ($CD14^+/CD66b^-$) subsets. (F) Quantitative analysis of respective FACS data for percentages of neutrophils ($CD66b^+$ cells) in healthy (HD-V1) and SCN patient (SCN-P12) differentiated HSCs that were mock-treated (Mock, black) or treated with RNP(alt) (gray). (n=3 groups of cells from HD-V1 healthy /SCN-P12 patient donors). Statistical significance is indicated as **P<.01, ***P<.001. (G) Quantitative analysis of respective FACS data for percentages of monocytes ($CD14^+/CD66b^-$ cells) in healthy (HD-V1) and SCN patient (SCN-P12) differentiated HSCs that were mock-treated (Mock, black) or treated with RNP(alt) (gray). (n=3 groups of cells from HD-V1 healthy /SCN-P12 patient donors). Statistical significance is indicated as ****P<.0001, ns = Not statistically significant. (H) Quantification of percentages of Zymosan Green uptake by healthy (HD-V1) and SCN patient (SCN-P12) differentiated HSCs that were mock-treated (Mock, black) or treated with RNP(alt) (gray). Statistical significance is indicated as ***P<.001, ns = Not statistically significant. (I) Graph depicts real time change in light emission, relative light units (RLUs), from 200,000 Luciferase expressing bacterial cells incubated with differentiated neutrophils from healthy mock-treated (HD-V1, Mock; white square), patient mock-treated (SCN-12 Mock; crossed circle) or patient RNP(alt)-treated (SCN-P12 RNP(alt); triangle) HSCs compared to bacterial cells only control (e-coli, circle). Statistical significance for each one of the groups versus e-coli control at the last time point presented, when RLU levels reached plateau, is indicated as *P<.05, **P<.01, ***P<.001. Bars represent mean values with standard deviation.

Figure S14.

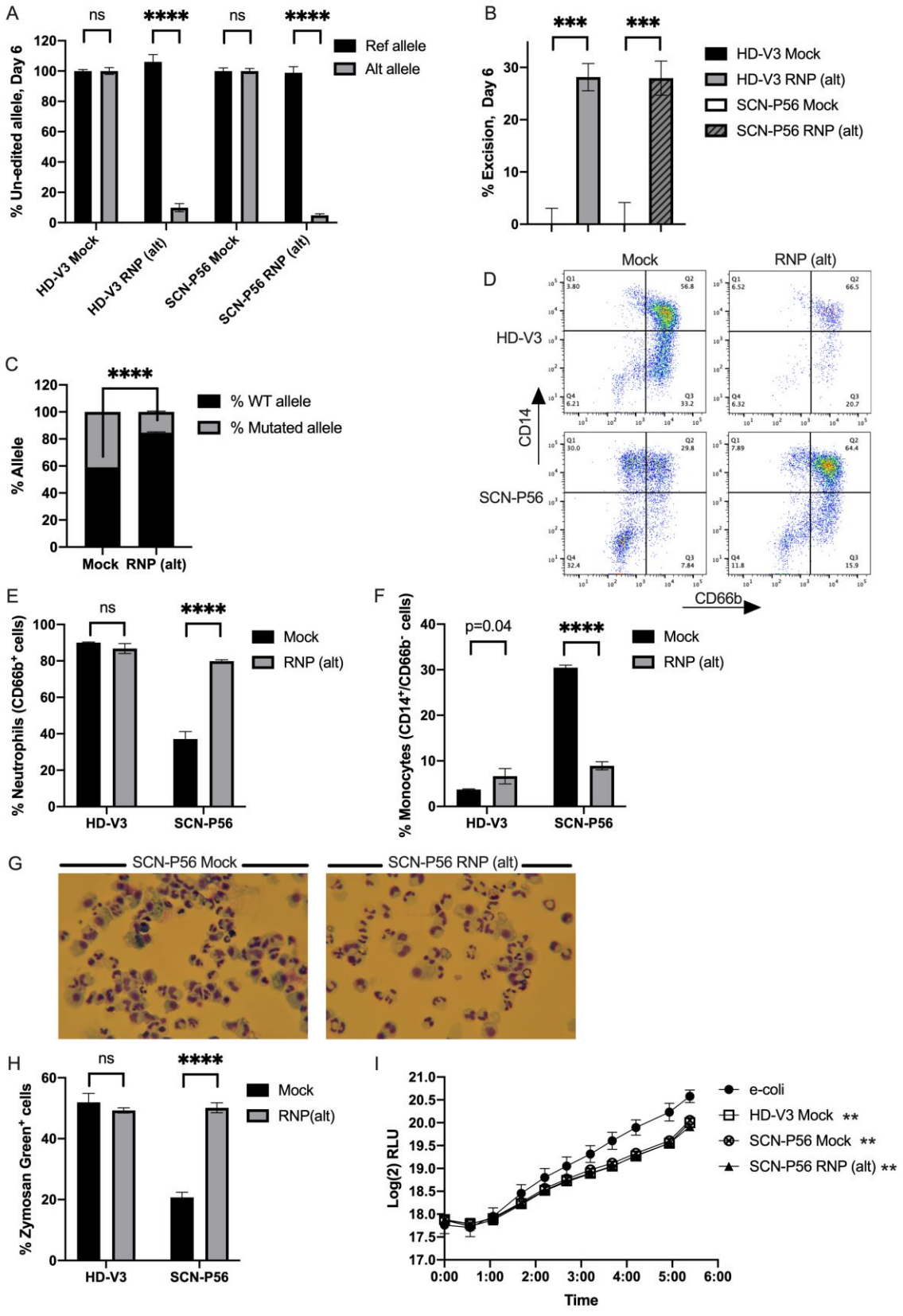
A
ns
****
ns
****
% Un-edited allele, Day 6
Ref allele
Alt allele
HD-V3 Mock
HD-V3 RNP (alt)
SCN-P56 Mock
SCN-P56 RNP (alt)
B
***
***
% Excision, Day 6
HD-V3 Mock
HD-V3 RNP (alt)
SCN-P56 Mock
SCN-P56 RNP (alt)
C
****
% Allele
% WT allele
% Mutated allele
Mock
RNP (alt)
D
Mock
RNP (alt)
HD-V3
SCN-P56
CD14
CD66b
E
ns
****
% Neutrophils (CD66b+ cells)
Mock
RNP (alt)
HD-V3
SCN-P56
F
p=0.04
****
% Monocytes (CD14+/CD66b- cells)
Mock
RNP (alt)
HD-V3
SCN-P56
G
SCN-P56 Mock
SCN-P56 RNP (alt)
H
ns
****
% Zymosan Green+ cells
Mock
RNP(alt)
HD-V3
SCN-P56
I
Log(2) RLU
e-coli
HD-V3 Mock **
SCN-P56 Mock **
SCN-P56 RNP (alt) **
Time

Figure S14. Excision using RNP(alt) in SCN-P56 and HD-V3. (A) Bar graphs representing percentages of un-edited reference (black) and alternative (gray) alleles at day 6 of differentiation in HSCs taken from either healthy donor (HD-V3) or SCN patient (SCN-P56) treated with RNP (alt) composition or electroporated without a nuclease composition (Mock), as measured by ddPCR. (n=3 groups of cells from HD-V3 healthy/SCN-P56 patient donors). Statistical significance is indicated as ****P<.0001, ns = Not statistically significant. (B) Bar graphs representing percentages of excision at day 6 of differentiation in HSCs taken from either healthy donor (HD-V3): Mock-treated (Mock, black) or RNP (alt)-treated (gray), or SCN patient (SCN-P56): Mock-treated (Mock, white) or RNP (alt)-treated (dark oblique lines), as measured by ddPCR. (n=3 groups of cells from HD-V3 healthy /SCN-P56 patient donors). Statistical significance is indicated as ***P<.001. (C) Bar graphs representing percentages of wild-type (black) and mutated (gray) alleles in cDNA taken from SCN-P56 patient HSCs that were either RNP (alt)-treated or Mock-treated (Mock), as measured by NGS targeting the mutation site. (n=3 groups of cells from SCN-P56 patient). Statistical significance is indicated as ****P<.0001. (D) Representative FACS plots of mock-treated (Mock, left panel) and RNP(alt)-treated (right panel) healthy donor (HD-V3, upper panel) and SCN-P56 patient (lower panel) differentiated HSCs, analyzed for neutrophilic ($CD66b^+$) and monocytic ($CD14^+/CD66b^-$) subsets. (E) Quantitative analysis of respective FACS data for percentages of neutrophils ($CD66b^+$ cells) in healthy (HD-V3) and SCN patient (SCN-P56) differentiated HSCs that were mock-treated (Mock, black) or treated with RNP(alt) (gray). (n=3 groups of cells from HD-V3 healthy /SCN-P56 patient donors). Statistical significance is indicated as ****P<.0001, ns = Not statistically significant. (F) Quantitative analysis of respective FACS data for percentages of monocytes ($CD14^+/CD66b^-$ cells) in healthy (HD-V3) and SCN patient (SCN-P56) differentiated HSCs that were mock-treated (Mock, black) or treated with RNP(alt) (gray). (n=3 groups of cells from HD-V3 healthy /SCN-P56 patient donors). Statistical significance is indicated as P=0.04, ****P<.0001. (G) Diff-Quik staining of P56 SCN patient-derived differentiated HSCs treated with RNP(alt) or electroporated without a nuclease composition (SCN-P56 Mock). Microphotographs were taken on LEITZ LABORLUX S polarizing light microscope at 400X magnification using Nikon DSLR digital camera. (H) Quantification of percentages of Zymosan Green uptake by healthy (HD-V3) and SCN patient (SCN-P56) differentiated HSCs that were mock-treated (Mock, black) or treated with RNP(alt) (gray). Statistical significance is indicated as ****P<.0001, ns = Not statistically significant. (I) Graph depicts real time change in light emission, relative light units (RLUs), from 200,000 Luciferase expressing bacterial cells incubated with differentiated neutrophils from healthy mock-treated (HD-V3, Mock; white square), patient mock-treated (SCN-56 Mock; crossed circle) or patient RNP(alt)-treated (SCN-P56 RNP(alt); triangle) HSCs compared to bacterial cells only control (e-coli, circle). Statistical significance for each one of the groups versus e-coli control at the last time point presented, when RLU levels reached plateau, is indicated as **P<.01. Bars represent mean values with standard deviation.

Figure S15.

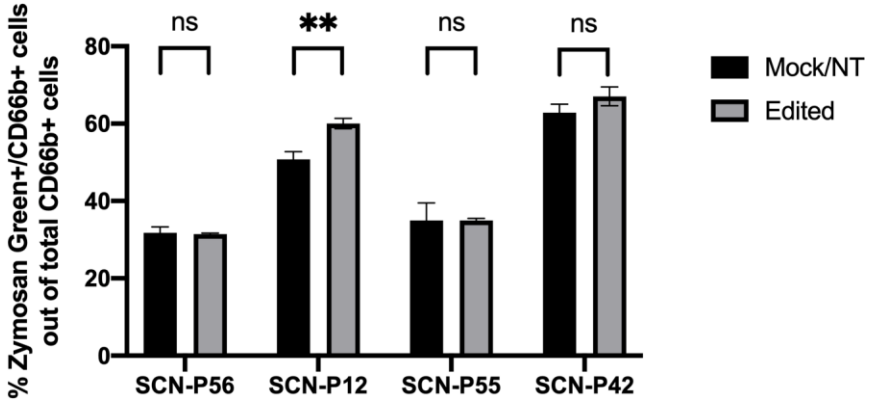

Figure S15. Phagocytosis out of total CD66b$^+$ cells. Quantification of percentages of Zymosan Green$^+$/CD66b$^+$ out of the total CD66b$^+$ neutrophils in patient-derived (SCN-P56, SCN-P12, SCN-P55 and SCN-P42) differentiated HSCs that were either mock/not-treated (black) or edited with RNP(alt)/(ref) (gray). Statistical significance is indicated as **P<.01, ns = Not statistically significant.

Table S1. Coverage of the three SNPs by the patient population.

Patient #	Diagnosis	Source	ELANE mutation	Location of mutation	rs10414837	rs3761005	rs1683564
1	SCN	Bone Marrow	S126L	4	CC	TA	CC
2	SCN	Bone Marrow	G210V	5	CT	TT	CC
3	SCN	Bone Marrow	C55S	2	CC	TA	CC
4	SCN	Bone Marrow	G221ter	5	CC	TA	AA
5	SCN	Bone Marrow	D230fs	5	CC	AA	CC
6	SCN	Bone Marrow	A57T	2	CT	TA	AA
7	SCN	Bone Marrow	R103P	3	CC	TT	AA
8	SCN	Bone Marrow	T128del	4	CT	AA	CA
9	SCN	Bone Marrow	V83D	3	CT	TT	AA
10	SCN	Bone Marrow	L84P	3	CT	TA	CA
11	SCN	Bone Marrow	L84P	3	CT	TT	CA
12	SCN	Bone Marrow	M154R	4	CC	TT	CA
13	SCN	Bone Marrow	G221ter	5	CT	TT	AA
14	SCN	Bone Marrow	G203R	5	CT	TA	CA
15	SCN	Bone Marrow	G214R	5	CC	AA	CA
16	SCN	Bone Marrow	P139L	4	CC	TA	CC
17	SCN	Bone Marrow	Y228ter	5	CT	TT	AA
18	SCN	Bone Marrow	P139L	4	CC	TA	CA
19	SCN	Bone Marrow	W156R	4	CT	TA	CC
20	SCN	Bone Marrow	P139L	4	CC	AA	CA
21	CyN	iPSC	P139L	4	CC	TT	CC
22	SCN	iPSC	I120N	3	CT	TT	AA
23	SCN	iPSC	G214R	5	CC	TA	CC
24	CyN	iPSC	S46F	2	CC	TA	CA
25	SCN	Bone Marrow	IVS4 +5G>A	INT4	CC	TT	CA
26	SCN	Bone Marrow	S126L	4	CC	TA	CA
27	SCN	Bone Marrow	R103L	3	CC	TA	CA
28	SCN	Bone Marrow	M66R	2	TT	TT	CC
29	SCN	Bone Marrow	C208X	5	CT	TA	CC
30	SCN	Bone Marrow	M1R	1	CC	TT	CA
31	SCN	Bone Marrow	P234fs	5	CC	AA	CC
32	SCN	Bone Marrow	I60T	2	CC	TT	CA
33	CyN	iPSC	IVS4 +1sd	INT4	CT	TT	CC
34	SCN	iPSC	P139L	4	CT	TT	AA
35	SCN	iPSC	R191S	4	TT	TT	CC
41	SCN	Bone Marrow	S126L	4	CC	AA	CA
42	SCN	Bone Marrow	S126L	4	CC	AA	CA
43	CyN	Bone Marrow	IVS4 +5 G>A	INT4	CC	TT	CC
44	CyN	Bone Marrow	IVS4 +1 G>A	INT4	CT	TA	CA
45	CyN	Bone Marrow	R220Q	5	CT	TT	CC
46	CyN	Bone Marrow	IVS4 +3 A>T	INT4	CC	TA	CC
47	CyN	Bone Marrow	W241ter	5	CT	AA	CC
48	SCN	Bone Marrow	S126L	4	CT	TA	CC
49	SCN	Bone Marrow	S126L	4	CT	TA	CC
50	SCN	Bone Marrow	P139L	4	CT	TA	CC
51	SCN	Bone Marrow	S46F	2	CC	TA	CC
52	SCN	Bone Marrow	IVS3 -8	INT3	CT	TA	CC
53	SCN	Bone Marrow	P139L	4	CC	TA	CA
54	SCN	Bone Marrow	R220Q	5	CC	TA	CA
55	SCN	Bone Marrow	R220Q	5	CT	TA	CA
56	SCN	Bone Marrow	A57V	2	CT	AA	CA
57	SCN	Bone Marrow	R191S	4	TT	TT	CC
58	CyN	Bone Marrow	S126L	4	CC	AA	CA

Sequencing results of the three SNPs in ELANE gene in samples obtained from SCN and Cyclic Neutropenia (cyN) patients. The pathogenic mutations in ELANE gene were also verified by sequencing. Green cells depict heterozygous SNPs.

Table S2. GUIDE-seq raw data.
Raw data from an unbiased survey (GUIDE-seq) of whole-genome off-target cleavage using OMNI A1 V10 nuclease and each of the constant guide (SgRNA(constant)), reference guide (SgRNA(ref)) and alternative guide (SgRNA(alt)).

Supplemental Methods

Human cells

Study approval was attained from Institutional Review Board of the University of Washington. Informed written consent was obtained from all the subjects of this study. Bone marrow samples were collected in association with an annual follow-up as recommended by the Severe Chronic Neutropenia International Registry.

Human SCN Patient HSC isolation

Three to 6 mls of freshly collected bone marrow was shipped overnight at ambient temperature. Hematopoietic stem and progenitor cells, HSPC's, were initially enriched using RosetteSep Human Bone Marrow Progenitor Cell Pre-Enrichment Cocktail, (Cat. No.15027) and Lymphoprep (Cat.no. 07801) according to manufacturer's protocol. The HSC enriched cell population was expanded by culturing for 4 days in $CD34^+$ expansion media (StemSpan SFEMII media (Cat.no. 09655) supplemented with 1% Penn Strep (Cat.no 03-031-1B, Biological Industries), 1x StemSpan CD34 Expansion Supplement(10x) (Cat.no. 02691), and 1.0µM UM729 (Cat.no.72332), at 37°C 5% CO_2. After expansion, $CD34^+$ cells were further enriched using EasySep Human CD34 Positive Selection Kit II (Cat.no. 17856) according to manufacturer's protocol. Enriched $CD34^+$ cells were cryopreserved at $1x10^6$ cells/ml in Cryostor CS10 (cat.no. 07931). Cells were stored in liquid nitrogen, vapor phase. All catalog numbers refer to materials from StemCell Technologies unless indicated otherwise. Patients used in this study were: SCN-P41 and SCN-P42, harboring the S126L mutation in exon 4 and SCN-P12 harboring the M154R mutation in exon 4, both mutations are linked to the reference form of the rs1683564 SNP, and SCN-P55 harboring the R220Q mutation in exon 5 and SCN-P56 harboring the A57V mutation in exon 2, both mutations are linked to the alternative form of the rs1683564 SNP.

Human healthy donor HSC isolation

Cryopreserved healthy human $CD34^+$ progenitor cells from mobilized peripheral blood were obtained from Lonza (Cat no. 4Y-101C). Cells were suspended in $CD34^+$ expansion media at 50,000 cells/ml and expanded for 4 days at 37°C, 5% CO_2 prior to electroporation.

Heterozygosity frequency of SNPs in the healthy and patient populations

Variant call files encompassing the *ELANE* gene region (± 3 kb of *ELANE* gene) were downloaded from the 1000 Genomes Project Consortium (phase 3) using the Data Slicer tool and analyzed in the R statistical computing environment. 3501 genotypes were available from 3501 individuals. Familial relationship was omitted from the analysis, which resulted in 2407 genotypes from unrelated individuals. The allele frequency for all common polymorphism (>1% MAF) was calculated. Three SNPs were chosen (rs3761005, rs1683564, and rs10414837 polymorphisms) to optimize the population coverage for allele-specific *ELANE* knock-out. The percentage of the population being heterozygous for at least one of the three chosen SNPs was calculated.

53 patients' samples were sequenced for the pathogenic mutation and the three chosen SNPs. A total of 46 bone marrow samples and 7 iPSC lines were used. 44 of the samples were from SCN patients and nine of them were from patients with Cyclic Neutropenia. Heterozygosity frequency of each of the three chosen SNPs and the percentage of the population being heterozygous for at least one of them was calculated.

CRISPR-associated OMNI A1 V10 *ELANE* gene editing

Editing of HSCs was carried out using a ribonucleic protein (RNP) system at a molar ratio of 1:2.5 (nuclease: sgRNA), including 17µg nuclease and 262pmol of each guide. Nuclease and sgRNA complex were incubate at 25°C for 10 minutes. Human $CD34^+$ cells were washed once with PBS. $2x10^5$ $CD34^+$ cells were suspended into 20µl of P3 electroporation buffer (Lonza P3 kit S) and were added to RNPs mix. After electroporation, using the CA-137 program (Lonza 4D, Nucleofector™), the cells were transferred to pre-warmed $CD34^+$ expansion media at a concentration of 1.25×10^5 cells/ml. Guides were manufactured by Agilent. Guide sequences are summarized in table S3.

Table S3. Guide sequences.

sgRNA name	Guide sequence (scaffold + spacer)
sgRef	GUGUCAAGCCCCAGAGGCCACAgUUUGAGAGUUAUGAAAAUGACGAGUUCAAA UAAAAAUUUAUUCAAACCGCCUAUUUAUAGGCCGCAGAUGUUCUGCUUU
sgAlt	GUGUCAAGCCCCAGAGGACACAgUUUGAGAGUUAUGAAAAUGACGAGUUCAAA UAAAAAUUUAUUCAAACCGCCUAUUUAUAGGCCGCAGAUGUUCUGCUUU

sgConstant	GCAGUCCGGGCUGGGAGCGGGUgUUUGAGAGUUAUGAAAAUGACGAGUUCAAA UAAAAAUUUAUUCAAACCGCCUAUUUAUAGGCCGCAGAUGUUCUGCUUU

OMNI A1 V10 is an engineered form of the newly discovered OMNI A1, a novel CRISPR nuclease of 1370 amino acids and an NGG PAM. OMNI-A1 was subjected to iterative rounds of mutagenesis followed by positive and negative selections (as described in Chen Z and Zhao H.[1] and Kleinstiver BP, et al.[2]) The resultant V10 nuclease, used in the current research, showed superior allele and target specificity, and had four amino acid substitutions relative to the original OMNI A1. One of the mutations is located at the REC1 domain and another one at the REC3 domain, suggesting potential interactions with the sgRNA and target DNA.

Digital Droplet PCR for percentage excision and allele specificity

Percentage excision and allele specificity were measured using Digital Droplet PCR™ (ddPCR™, Bio-Rad, Hercules, CA, USA) on genomic DNA that was extracted using QIAamp DNA Micro Kit, Qiagen (Cat no. 56304). According to manufacturer's protocol.

ddPCR reaction contained 1× ddPCR Supermix for probe without dUTP (#1863024), 25-100ng of digested DNA using HindIII (diluted in X1 Cutsmart Buffer to 4U/μL) and suitable primers/probes. For excision reaction, amplification of two regions in *ELANE* gene, exon 1 and exon 5 was performed, using two different probes labeled with FAM (X1) and HEX (X1), respectively. The ratio between the HEX and the FAM signals was translated to excision efficiency. The location of the probes is presented in Figure S16. The same probes can be used for the strategies based on the upstream SNPs (rs10414837 and rs3761005).

For allele specificity, two competitive probes: a FAM probe, which binds the alternative allele, and a HEX probe, which binds the reference allele were used (FAM+HEX). The ratio between the concentrations of the two in heterozygote non-treated cell is 1, which was normalized to the endogenous genes RPP30 and STAT1 for each gDNA sample. Reaction total volume was 22μL. The binding of each probe to DNA extracted from healthy donor cells that were homozygous to either the reference or alternative forms of the SNP was measured by ddPCR, confirming the probes do not cross react, (**Figure S5A**). Moreover, healthy donor cells homozygous to the reference form of the SNP depicted efficient excision when treated with RNP(ref) composition, compared to treatment with RNP(alt) composition that resulted in excision levels comparable to non-treated cells. This further demonstrates the specific targeting of the sgRNAs (**Figure S5B**).

Genomic DNA in the ddPCR mixture was partitioned into individual droplets using QX100 Droplet Generator, transferred to a 96-deep well PCR plate and amplified in a Bio-Rad PCR thermocycler. Bio-Rad Droplet Reader and QuantaSoft Software were used to read and analyzed the experiment following manufacturer's guidelines (Bio-Rad). The primers and probes were manufactured by Bio-Rad and are detailed in table S4.

Table S4. Primers and probes for excision and allele specificity measurements.

Probe name	Catalog number
ELANE ddPCR assay Exon1 (FAM)	dHsaCNS328407057
ELANE ddPCR assay Exon5 (HEX)	qHsaCEP0055470
rs1683564 Editing ddPCR assay (FAM+HEX)	dHsaMDS873573221
RPP30	dHsaMDS117591774
STAT1	dHsaCNS850507320

Figure S16.

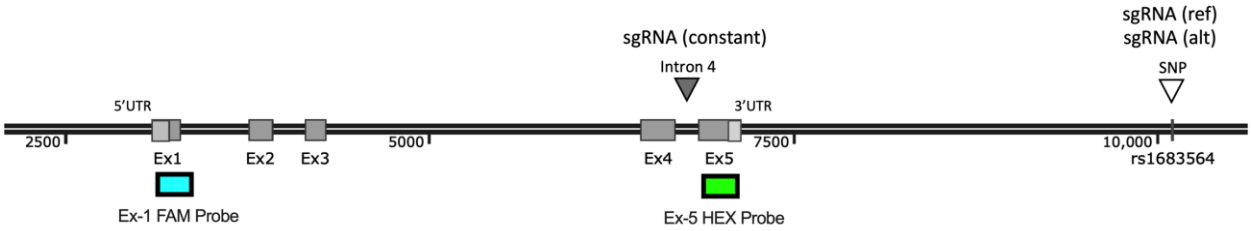

Figure S16. Location of FAM and HEX probes used to determine excision.

Assessment of mutated/wild-type allele ratio

cDNAs from HSCs treated with either RNP(ref) or RNP(alt), mock-treated or not-treated were mapped using next-generation sequencing (NGS) targeting exon 4 (for patients 41 and 42 (harboring the S126L mutation) and patient 12 harboring the M154R mutation), exon 5 (for patient 55 harboring the R220Q mutation) and exon 2 (for patient 56 harboring the A57V mutation). The raw FASTQ files were analyzed, and BAM files (text-based format for storing biological sequences) were generated using FASTQ to BAM script. The relative ratio of the mutated allele to the wild-type allele was calculated and compared to the non-treated or mock-treated cells in all patients. This assay was used as a robust approach targeting the exons that harbor the mutations, instead of addressing each mutation individually (as SCN is associated with more than 200 different mutations in *ELANE*). The primers used in this assay are suitable for several patients as detailed in table S5.

Table S5. Primers used for assessment of mutated/wild-type allele ratio.

Mutation	Sequence
S126L (P41, P42); M154R, (P12)	TCGTCGGCAGCGTCAGATGTGTATAAGAGACAGNNNTACGACCCCGTAAACTTGCT GTCTCGTGGGCTCGGAGATGTGTATAAGAGACAGNNNCGGAGCGTTGGATGATAGAG
R220Q (P55)	TCGTCGGCAGCGTCAGATGTGTATAAGAGACAGNNNTCGCAGTCCAGCTTCCCCAC GTCTCGTGGGCTCGGAGATGTGTATAAGAGACAGNNNACAGCCAAGGAGCATCAAAC
A57V (P56)	TCGTCGGCAGCGTCAGATGTGTATAAGAGACAGNNNCCCTTCATGGTGTCCCTGC GTCTCGTGGGCTCGGAGATGTGTATAAGAGACAGNNNCCGTCACGTTGAGCTCCTG

ddPCR *ELANE* expression assay

RNA purification.

Pellets of fresh, day 6 differentiated HSCs centrifuged at 300 g for 5 min and kept on ice were used. Total RNA was extracted using RNeasy® Mini Kit according to the manufacturer's instructions (QIAGEN #74104) with 600 µl RTL supplemented with β-Mercaptoethanol and on-column DNAseI treatment for 30 min. Total RNA concentration was determined by NanoDrop and RNA integrity number equivalent (RINe) of samples was determined by TapeStation according to Agilent RNA ScreenTape Quick Guide for TapeStation Systems (Agilent, Publication Part Number: G2991-90021). RNA samples had RINe > 8.0.

ELANE mRNA expression levels estimate

RNA was purified from patient HSCs excised with either RNP(ref) or RNP (alt), mock-treated or not-treated, as described. cDNA was prepared using High-Capacity RNA-to-cDNA kit according to the manufacturer's instructions (Applied Biosystems, #4387406), normalized to 10 pg/µl initial RNA and stored at -20°C until use. For each sample, a no reverse transcriptase control was also prepared with ultra-pure water instead of reverse transcriptase to ensure there is no gDNA contamination. For each of the cDNA samples, a PCR master mix of 2x QX200 ddPCR EvaGreen® Supermix (10 µl per reaction, Bio-Rad, 1864033) and cDNA (6 µl per reaction, 60 pg initial RNA) was prepared according to the number of reactions needed (2 technical repeats per each target plus 1 extra reaction to account for pipetting errors). For each PCR reaction, the master mix (16 µl) was dispensed into reaction tubes prior to adding forward and reverse primers mix (500 nM, 4 µl) specific to the target. For each of the targets, a no template control reaction with ultra-pure water instead of cDNA was included to ensure there is no primer dimer

formation or extraneous nucleic acid contamination. Primers used are detailed in table S6.

Table S6. Primer sequences for measuring *ELANE* expression levels by ddPCR.

Gene	Forward primer sequence	Reverse Primer sequence
ELANE	CTACGACCCCGTAAACTTGCT	CCGACCCGTTGAGCTGGAG
GAPDH	CATCACCATCTTCCAGGAGCGAG	CCCCTGCAAATGAGCCCCAG

PCR-ready samples were loaded into DG8 cartridges and droplets were generated according to the QX200 Droplet Generator Instruction Manual (Bio-Rad, Bulletin# 10031907). The droplets were transferred into a 96-well ddPCR plate according to the experiment pre-designed plate layout. The plate was sealed with a pierceable foil heat seal according to the PX1TM PCR Plate Sealer Instruction Manual (Bio-Rad, Bulletin# 10023997). The PCR-ready plate was placed into Bio-Rad's C1000 Touch Cycler for PCR amplification according to Table 2. Thermal Cycling Protocol in the ddPCR Gene Expression EvaGreen® Assays Product Insert (Bio-Rad, Bulletin# D107737) with annealing/extension at 59°C. The post-PCR plate was placed into the QX200 Droplet Reader. Setup, Run, and analyze were preformed according to the QX200 Droplet Reader and QuantaSoft Software Instruction Manual (Bio-Rad, Bulletin# 10031906). For Setup, ABS (Absolute Quantification) option for Experiment and the QX200 ddPCR EvaGreen Supermix option for Supermix were used. Run followed as described in the manual. For Analyze, the concentration data, number of events, and the thresholds were reviewed for each of the wells in the QuantaSoft Software. Thresholds were adjusted, if needed, and the results exported to Excel. For each well, the average concentration and standard deviation of the 2-technical repeats of each of the targets was calculated. Wells with anomalous values, such as too few droplets or high standard deviation between the technical repeats, were omitted from the analysis. For each biological sample, ELANE mRNA expression levels were normalized to the GAPDH mRNA levels. Then, the ELANE normalized levels were normalized to the average of ELANE normalized levels of the mock or NT samples, as follows:

$$\frac{ELANE\ average\ copies/\mu l}{GAPDH\ average\ copies/\mu l} = ELANE\ normalized\ levels$$

$$\frac{ELANE\ normalized\ levels}{Average\ of\ ELANE\ normalized\ levels\ of\ the\ MOCK/NT\ samples} = ELANE\ mRNA\ ratio$$

Differentiation assay

Edited and non-treated or mock-treated HSCs were allowed to recover for 3 days in $CD34^+$ expansion media and were subjected to a differentiation protocol adopted from Nasri et al.[3] In brief, HSCs were cultured for 7 days in RPMI (Cat.no 11875093, Gibco™) supplemented with 1% Glutamax (Cat.no 35050061, Gibco™), 10% FBS (Cat.no 04-001-1A, Biological Industries), 5ng/ml IL-3 (Cat.no 200-03), SCF (Cat.no 300-07), GM-CSF (Cat.no 300-03) & 10ng/ml G-CSF (Cat.no 300-23), all from PeproTech, for proliferation and myeloid progenitor differentiation followed by a 7-day culture in RPMI , 1% Glutamax, 10% FBS, 1% Penn Strep (Cat.no 03-031-1B, Biological Industries), 10ng/ml G-CSF for neutrophil differentiation and maturation. On day 14 cells were analyzed by flow cytometry for monocytic ($CD14^+/CD66b^-$) and neutrophilic ($CD66b^+$ or $CD11b^+/CD15^+$) subsets. CD66b anti-human; Pacific Blue (Cat No. 305112, Biolegend), CD14 anti-human; APC (Cat No. 130-110-520), CD11b anti-human; APC (Cat No. 130-110-554) and CD15 anti-human; Pacific Blue (Cat No. 130-113-488) all from Miltenyi Biotec, unless indicated otherwise, were used.

Cytospin staining

$8x10^4$ HSCs at day 15 of differentiation were spun onto Cytoslide microscope slides (ThermoFisher) using Cytospin 4 low speed cytocentrifuge (Thermo Scientific) and stained with Diff-Quick staining system (MilliporeSigma) according to manufacturer's recommendations. Microphotographs were taken on LEITZ LABORLUX S polarizing light microscope at 400X magnification using Nikon DSLR digital camera.

Bacterial killing assay

Day 13 differentiated HSCs (subjected to a differentiation protocol adopted from Nasri et al.[3]) from healthy donors and SCN patients (edited with either RNP(ref), RNP(alt), mock-treated or non-treated), were evaluated for their bacterial killing capacity as described in J. T. Atosuo.[4] Briefly, 100,000 differentiated HSCs were incubated in the

presence of 200,000 Luciferase expressing bacterial cells, pAKLUX2, per well (Addgene, Cat No. 14080)[5]. Cells were cultured in 200 µl HBSS++, 10% FBS at 37°C. At 30-minute intervals luminescence was measured by transferring the plate to a Luminometer (Berthold CentroXS3 LB960) and measuring luminescence for 0.5 sec per well). A real time change in light emission, relative light units (RLUs), was measured over 5 hrs. Last time point presented is when RLU levels reached plateau. Wells without differentiated HSCs (E.coli only) and with 10ng/ml phagocytosis inhibitor (data not shown), Cytochalasin D (Santa Cruz Biotec, Cat No. sc-20144) served as controls. pAKlux2 was a gift from Attila Karsi (Addgene plasmid # 14080; http://n2t.net/addgene:14080 ; RRID:Addgene_14080).

Phagocytosis assay

Phagocytosis capacity was evaluated using the EZCell™ Phagocytosis Assay Kit (Green Zymosan), (BioVision, Cat no. K397 according to manufacturer's protocol). Day 14 differentiated HSCs (subjected to a differentiation protocol adopted from Nasri et al.[3]) from healthy donors and SCN patients (edited with either RNP(ref), RNP(alt), mock-treated or non-treated), were resuspended in HBSS++/10% FBS ($0.5X10^6$ cells/ml) and incubated for 1.5 hours at 37°C in the presence of 5ml opsonized Alexa Fluor 488-conjugated zymosan particles per 200ml suspended cells. As a negative control, cells were incubated with 10ng/ml of the phagocytosis inhibitor, Cytochalasin D (Santa Cruz Biotec, Cat No. sc-201442) 1 hour prior and during incubation with Zymosan Green reagent. Cells were then washed and incubated in a quencher solution, based on kit's instructions, to remove fluorescence from particles that were not internalized. Cells were then analyzed by flow cytometry for internalization of opsonized fluorescent Zymosan Green particles.

Editing at upstream SNPs

Genomic DNAs from U2OS cells (ATCC), treated with non-engineered OMNI-A1 and either sgRNA 39 (targeting rs10414837 SNP) or sgRNA 58 (targeting rs3761005 SNP), were mapped using next-generation sequencing (NGS) with PCR amplicons spanning the sgRNA genomic target sites (SNPs rs10414837 or rs3761005) to measurer genetic variation due to editing. For gene specific PCR, we used NEBNext® Ultra™ II Q5® Master Mix (NEB, #M0544) with the primers listed in table S7.

Table S7. Primers used to measure editing at upstream SNPs.

ELANE_g39 rs10414837	FP: TCGTCGGCAGCGTCAGATGTGTATAAGAGACAGNNNGGTGGGTCCTCAGTGACTCT RP: GTCTCGTGGGCTCGGAGATGTGTATAAGAGACAGNNNGGGAATTCCAGCCTGACCAA
ELANE_g58 rs3761005	FP: TCGTCGGCAGCGTCAGATGTGTATAAGAGACAGNNNGAGTGAGGACCAAGCCTGAG RP: GTCTCGTGGGCTCGGAGATGTGTATAAGAGACAGNNNAGGGCCATTGTCTCCCTAAC

The indexing PCR was performed with illumina Nextera index sets. The generated library was sequenced with illumina NextSeq SR150 and the FASTQ files were analyzed with CRISPRESSO2 pipeline.[6]

Inversions

Inversion events were detected and quantified by a Droplet Digital PCR (ddPCR) mutation assay. First, a perfect inversion was mimicked using a SnapGene software and verified by NGS.
Then, total inversion events were quantified by ddPCR using EvaGreen dye, a fluorescent DNA-binding dye that binds dsDNA (BIO-RAD, catalog number 186-4034, according to manufacturer's protocol). Specific primers were designed to amplify inverted variations of the excised fragment (See illustration in Figure S6). Fluorescent signals were normalized to amplification of *ELANE* exon 1 region that was not affected by excision (performed by two different sets of primers. Averaged normalized data is presented). Primers are detailed in table S8.

Table S8. Primers used to detect and quantify inversion events.

Primer name	Sequence
Exon 4 primer	ACGTCTGCACTCTCGTGAGG
Exon 5 primer (inverted)	TTCAGGCTCCACCCAGTTTGTC

Exon 1 primers	Mix3: GCACAGGGCTATAAGAGGAGC GCGGGAGGTTGGACTCAAAA
	Mix6: GGGAGAGGAAGTGGAGGGC GAGGGTCATGGTGGGGCT

Excision levels in Long Term HSC population

HSCs of two healthy donors (MLP1 (3055934); heterozygous to the alternative form of the SNP and MLP2 (3055940), homozygous to the alternative form of the SNP), isolated from leukopaks purchased from AllCells, were edited a day after thaw according to 'CRISPR-associated OMNI A1 V10 *ELANE* gene editing' section above, with minor changes. Cell number was 2M cells/electroporation. Upscale of guides and nuclease was performed accordingly. A molar ratio of 1:2.5 (nuclease: sgRNA) was used including 85µg nuclease and 1310 pmol of each guide. Nucleofection was performed in P3 nucleofection solution (Lonza) and Lonza 4D-Nucleofector™ X Kit L (program CA-137). Three days after editing, cells were sorted in a FACS ARIA™ II SORP Flow Cytometer Cell (BD), using CD90-APC-Vio770, human (130-114-863 Milteny). Sorted cells were incubated for 7 days in a proliferation medium according to Nasri et al.[3] Excision levels of $CD90^+$, $CD90^-$ and total population were evaluated using ddPCR as described in ddPCR section.

Mutation-SNP linkage

First, *ELANE* mutation and possible SNPs were identified in cells from SCN patients by targeted short read NGS. Then, a part of the gene encompassing both the mutation and the SNP was amplified by a PCR reaction with linkage primers and cloned into bacteria. Each clone bore an amplicon from one allele. A plasmid of multiple clones was Sanger sequenced (with T7 and SP6 primers) for the mutation and the SNP regions. If the mutation and the SNP were in cis, they were found at the same clone, if in trans, the mutation and SNP were found in different clones. Primers are detailed in table S9.

Table S9. Primers used for Mutation-SNP linkage assay.

Primer name	Sequence
rs10414837	FP: TCGTCGGCAGCGTCAGATGTGTATAAGAGACAGNNNGGTGGGTCCTCAGTGACTCT
	RP: GTCTCGTGGGCTCGGAGATGTGTATAAGAGACAGNNNGGGAATTCCAGCCTGACCAA
rs3761005	FP: TCGTCGGCAGCGTCAGATGTGTATAAGAGACAGNNNGAGTGAGGACCAAGCCTGAG
	RP: GTCTCGTGGGCTCGGAGATGTGTATAAGAGACAGNNNAGGGCCATTGTCTCCCTAAC
rs1683564	FP: TCGTCGGCAGCGTCAGATGTGTATAAGAGACAGNNNTCCTGCTACCCTCCCTTCTT
	RP: GTCTCGTGGGCTCGGAGATGTGTATAAGAGACAGNNNTTTTAGGAGGGGCCCACTGA
Linkage	FP: GAGGGTCATCATCACTGCCC
	RP: GCCAGACTCACACCAGAGTCGACAAGT
T7	TAATACGACTCACTATAGGG
SP6	ATTTAGGTGACACTATAG
R220Q mutation (SCN-P55)	FP: TCGTCGGCAGCGTCAGATGTGTATAAGAGACAGNNNTCGCAGTCCAGCTTCCCCAC
	RP: GTCTCGTGGGCTCGGAGATGTGTATAAGAGACAGNNNACAGCCAAGGAGCATCAAAC
S126L mutation (SCN-P41, SCN-P42)	FP: TCGTCGGCAGCGTCAGATGTGTATAAGAGACAGNNNGAGGGTCATCATCACTGCCC
	RP: GTCTCGTGGGCTCGGAGATGTGTATAAGAGACAGNNNAGTCCGGGCTGGGAGCGGGT
A57V mutation (SCN-P56)	FP: TCGTCGGCAGCGTCAGATGTGTATAAGAGACAGNNNCGCACACTCCCGGCTACTCA
	RP: GTCTCGTGGGCTCGGAGATGTGTATAAGAGACAGNNNCTCAGTTTCCTCATCTGAACAACAG

Analysis of off-targets

GUIDE-seq analysis was performed as described in Tsai et al[7] using 50pmol 46bp dsODN (ATATCGCGTCCGTTATTAACATATGACAACTCAATTAAACGCGAAC). NGS library preparation was done as in Palani's protocol[8]. For *in-silico* analysis, *Cas-Offinder* was used to identify potential off-targets of up to 3 mismatches for each of the guides. The off-target sites retrieved from *Cas-Offinder* were tested by rhAmpSeq analysis. The rhAmpSeq multiplex amplicon sequencing technology (IDT, Coralville, IA) was used to quantify off-target editing activity, the rhAmpSeq library for the targeted amplicons sequencing was prepared according to IDT's protocol.[9] The accuracy of the multiplex rhAmpSeq technology is based on blockage primers containing RNA bases at the 3′ end of the primer, causing DNA/RNA hybridization. A perfect DNA/RNA alignment is cleaved by RNase H2 enzyme, allowing continuance amplification. rhAmpSeq primers were designed using the IDT rhAmpseq design website[10] to flank each off-target cut-sites identified by Cas-Offinder and pooled together for multiplex assay amplification (IDT, Coralville, IA). The off-target panels were tested on HSCs derived from patients edited with RNP(ref) or RNP(alt). Each experiment was performed with three independent repeats. 100 ng DNA from each sample was submitted to a two-round rhAmpSeq PCR according to the manufacturing protocol. rhAmpSeq amplicons were purified and sequenced using the Illumina NextSeq platform (150-bp paired-end reads) and analyzed with IDT pipeline.

NETosis assay

HSCs taken from two healthy donors were either not-treated (NT), RNP(ref)-treated or RNP(alt)-treated and were subjected to a differentiation protocol as described above. 20,000 differentiated HSCs were seeded in a 96 well plate, in F-12 medium (Sartorius), a low auto-fluorescence media. Cells were stimulated with PMA (Sigma-Aldrich) (1000 nM) to induce NETosis or added with 0.1% DMSO (No PMA control). 250μM SYTOX Green dye (Sartorius), a high-affinity nucleic acid stain that easily penetrates cells with compromised plasma membranes was added for detection of membrane-damaged cells. Cells were imaged using phase contrast and green (300-ms exposure) channels in the Incucyte® S3 System, which was housed in a cell incubator at 37˚C with 5% CO_2. Three image sets from distinct regions per well were taken every 30 minutes for up to 10 hours. Each condition was run in triplicate. Cells undergoing NETosis were identified by green staining following membrane damage. For the green channel, edge sensitivity was set to -20, and hole fill was set to 30μm^2. A minimum area of 400μm^2 was set in the processing definition for exclusion of apoptotic cells that are also stained by the SYTOX Green dye, but to a much smaller area compared to NETotic cells. To determine the number of neutrophils per well, total number of

neutrophils were calculated according to phase images using adherent cell-by-cell analysis. To determine the percentage of cells undergoing NETosis, the green object count after 10-hour stimulus was divided by the total cell count at the starting time point. Data is presented as fold change relative to NT 1000nM PMA.

Statistical methods

The two-sample T-test for independent samples or the Anova model, as appropriate, was applied for testing the statistical significance of the difference in continuous variables between treatment groups. The two-ways Analysis of Variance with repeated measurements was used to analyze killing assays. Chi-square test or Fisher's Exact test, as appropriate, was applied to test the statistical significance of the difference in heterozygosity between healthy and patient populations. All tests were two-tailed, and a p-value of 5% or less was considered statistically significant. The data was analyzed using Prism software (GraphPad version 9.0.2).

References

1. Chen, Z., and Zhao, H. (2005). A highly sensitive selection method for directed evolution of homing endonucleases. Nucleic Acids Res. *33*, e154.

2. Kleinstiver, B.P., Prew, M.S., Tsai, S.Q., Topkar, V., Nguyen, N.T., Zheng, Z., Gonzales, A.P.W., Li, Z., Peterson, R.T., Yeh, J.-R.J., et al. (2015). Engineered CRISPR-Cas9 nucleases with altered PAM specificities. Nature *523*, 481–485.

3. Nasri, M., Ritter, M., Mir, P., Dannenmann, B., Aghaallaei, N., Amend, D., Makaryan, V., Xu, Y., Fletcher, B., Bernhard, R., et al. (2020). CRISPR/Cas9-mediated ELANE knockout enables neutrophilic maturation of primary hematopoietic stem and progenitor cells and induced pluripotent stem cells of severe congenital neutropenia patients. Haematologica *105*, 598–609.

4. Atosuo, J.T., and Lilius, E.-M. (2011). The Real-Time-Based Assessment of the Microbial Killing by the Antimicrobial Compounds of Neutrophils. ScientificWorldJournal *11*, 2382–2390.

5. Karsi, A., and Lawrence, M.L. (2007). Broad host range fluorescence and bioluminescence expression vectors for Gram-negative bacteria. Plasmid *57*, 286–295.

6. Clement, K., Rees, H., Canver, M.C., Gehrke, J.M., Farouni, R., Hsu, J.Y., Cole, M.A., Liu, D.R., Joung, J.K., Bauer, D.E., et al. (2019). CRISPResso2 provides accurate and rapid genome editing sequence analysis. Nat. Biotechnol. *37*, 224–226.

7. Tsai, S.Q., Zheng, Z., Nguyen, N.T., Liebers, M., Topkar, V.V., Thapar, V., Wyvekens, N., Khayter, C., Iafrate, A.J., Le, L.P., et al. (2015). GUIDE-seq enables genome-wide profiling of off-target cleavage by CRISPR-Cas nucleases. Nat. Biotechnol. *33*, 187–197.

8. Palani, N. (2018). GUIDE-seq simplified library preparation protocol (CRISPR/Cas9 off-target cleavage detection).

9. User guides & protocols Integr. DNA Technol. https://eu.idtdna.com/pages/support/guides-and-protocols.

10. rhAmpSeq™ Design Tool tutorial Integr. DNA Technol. https://www.idtdna.com/pages/education/videos/detail/rhampseq-design-tool-tutorial-video.